

Fig. 12. Neurotoxicity of CDDP and NC-6004 in rats. Rats ($n=5$) were given CDDP (2 mg/kg), NC-6004 (an equivalent dose of 2 mg/kg CDDP), or 5% glucose, all intravenously twice a week, 11 administrations in total. Sensory nerve conduction velocity (SNCV) and motor nerve conduction velocity (MNCV) of the sciatic nerve at week 6 after the initial administration (A). The platinum concentration in the sciatic nerve. Rats were given CDDP (5 mg/kg, $n=5$), NC-6004 (an equivalent dose of 5 mg/kg CDDP, $n=5$), or 5% glucose ($n=2$), all intravenously twice a week, 4 administrations in total. On day 3 after the final administration, a segment of the sciatic nerve was removed and the platinum concentration in the sciatic nerve was measured by ICP-MS (B). The data are expressed as the mean \pm S.D. *: $P < 0.05$ [39].

nerve conduction velocities (SNCVs) in animals given 5% glucose, CDDP, and NC-6004 were 42.86 ± 8.07 , 35.48 ± 4.91 , and 43.74 ± 5.3 m/s, respectively. Animals given NC-6004 showed no delay in SNCV as compared with animals given 5% glucose. On the other hand, animals given CDDP showed a significant delay ($P < 0.05$) in SNCV as compared with animals given NC-6004 (Fig. 12A). The analysis by ICP-MS on sciatic nerve concentrations of platinum could not detect platinum in the sciatic nerve from animals given 5% glucose (data not shown). Sciatic nerve concentrations of platinum in animals given CDDP and NC-6004 were 827.2 ± 291.3 and 395.5 ± 73.1 ng/g tissue. Therefore, the concentrations were significantly ($P < 0.05$) lower in animals given NC-6004 (Fig. 12B). This finding is believed to be a factor which reduced neurotoxicity following NC-6004 administration as compared with the CDDP administration.

3.6. Present situation of a clinical study of NC-6004

A phase 1 clinical trial of NC-6004 is now under way in United Kingdom. Starting dose of NC-6004 was 10 mg/m². NC-6004 was administered once every 3 weeks with only 1000 ml water loading. In Japan, a phase 1 trial will be started soon in the National Cancer Center Hospital.

4. NK012, SN-38-incorporating micellar nanoparticle

The antitumor plant alkaloid camptothecin (CPT) is a broad-spectrum anticancer agent which targets the DNA topoisomerase I. Although CPT has showed promising antitumor activity *in vitro* and *in vivo* [40,41], it has not been used clinically because of its low therapeutic efficacy and severe toxicity [42,43]. Among CPT analogs, irinotecan hydrochloride (CPT-11) has recently been demonstrated to be active against colorectal, lung, and ovarian cancer [44–48]. CPT-11 itself is a prodrug and is converted to 7-ethyl-10-hydroxy-CPT (SN-38), a biologically active metabolite of CPT-11, by carboxylesterases (CEs). SN-38 exhibits up to 1000-fold more potent cytotoxic activity against various cancer cells *in vitro* than CPT-11 [49]. Although CPT-11 is converted to SN-38 in the liver and

tumor, the metabolic conversion rate is less than 10% of the original volume of CPT-11 [50,51]. In addition, the conversion of CPT-11 to SN-38 depends on the genetic inter-individual variability of CE activity [52]. Thus, direct use of SN-38 might be of great advantage and attractive for cancer treatment. For the clinical use of SN-38, however it is essential to develop a soluble form of water-insoluble SN-38. The progress of the manufacturing technology of “micellar nanoparticles” may make it possible to use SN-38 for *in vivo* experiments and further clinical use.

4.1. Preparation and characterization of NK012

NK012 is an SN-38-loaded polymeric micelle constructed in an aqueous milieu by the self-assembly of an amphiphilic block copolymers, PEG-PGlu(SN-38) [53]. The molecular weight of PEG-PGlu(SN-38) was determined to be approximately 19,000 (PEG segment: 12,000; SN-38-conjugated PGlu segment: 7,000). NK012 was obtained as a freeze-dried formulation and contained ca. 20% (w/w) of SN-38 (Fig. 13A). The mean particle size of NK012 is 20 nm in diameter with a relatively narrow range (Fig. 13B). The releasing rates of SN-38 from NK012 in phosphate buffered saline at 37 °C were 57% and 74% at 24 h and 48 h, respectively, and that in 5% glucose solution at 37 °C were 1% and 3% at 24 h and 48 h, respectively (Fig. 13C). These results indicate that NK012 can release SN-38 under neutral condition even without the presence of a hydrolytic enzyme, and is stable in 5% glucose solution. It is suggested that NK012 is stable before administration and starts to release SN-38, the active component, under physiological conditions after administration.

4.2. Cellular sensitivity of NSCLC and colon cancer cells to SN-38, NK012, and CPT-11

The IC₅₀ values of NK012 for the cell lines ranged from 0.009 μM (Lovo cells) to 0.16 μM (WiDR cells). The growth-inhibitory effects of NK012 are 43–340-fold more potent than those of CPT-11, whereas the IC₅₀ values of NK012 were 2.3–5.8-fold higher than those of SN-38. NK012 exhibited a higher

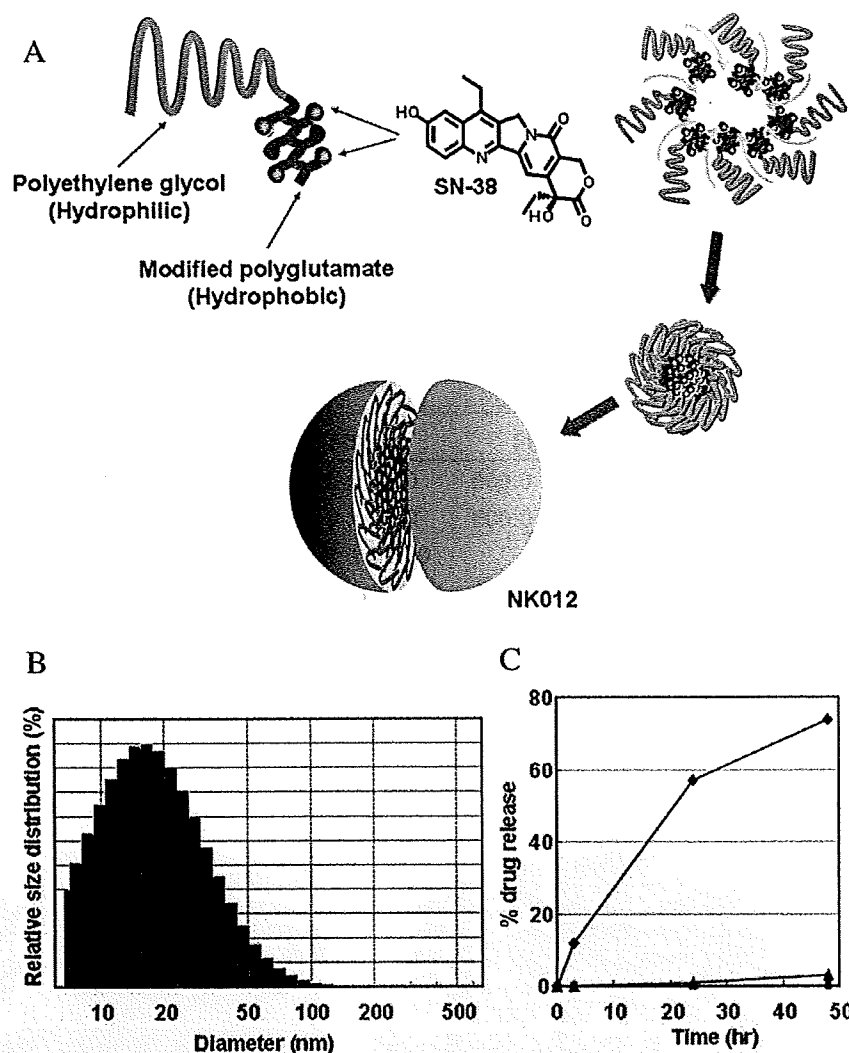


Fig. 13. Schematic structure of NK012. A polymeric micelle carrier of NK012 consists of a block copolymer of PEG (molecular weight of about 5000) and partially modified polyglutamate (about 20 unit). Polyethylene glycol (hydrophilic) is believed to be the outer shell and SN-38 was incorporated into the inner core of the micelle [56].

cytotoxic effect against each cell line as compared with CPT-11 ($\times 43$ – 340 -fold sensitivity). On the other hand, the IC_{50} values of NK012 were a little higher than those of SN-38, similar to the cytotoxic feature also reported in a previous study about micellar drugs [39].

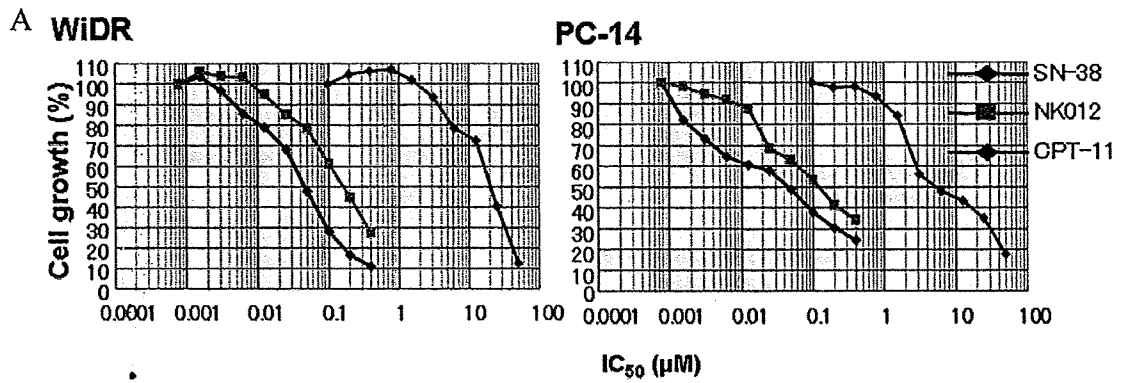
4.3. Pharmacokinetic analysis of NK012 and CPT-11 using HT-29-bearing nude mice

After injection of CPT-11, the concentrations of CPT-11 and SN-38 for plasma declined rapidly with time in a log-linear

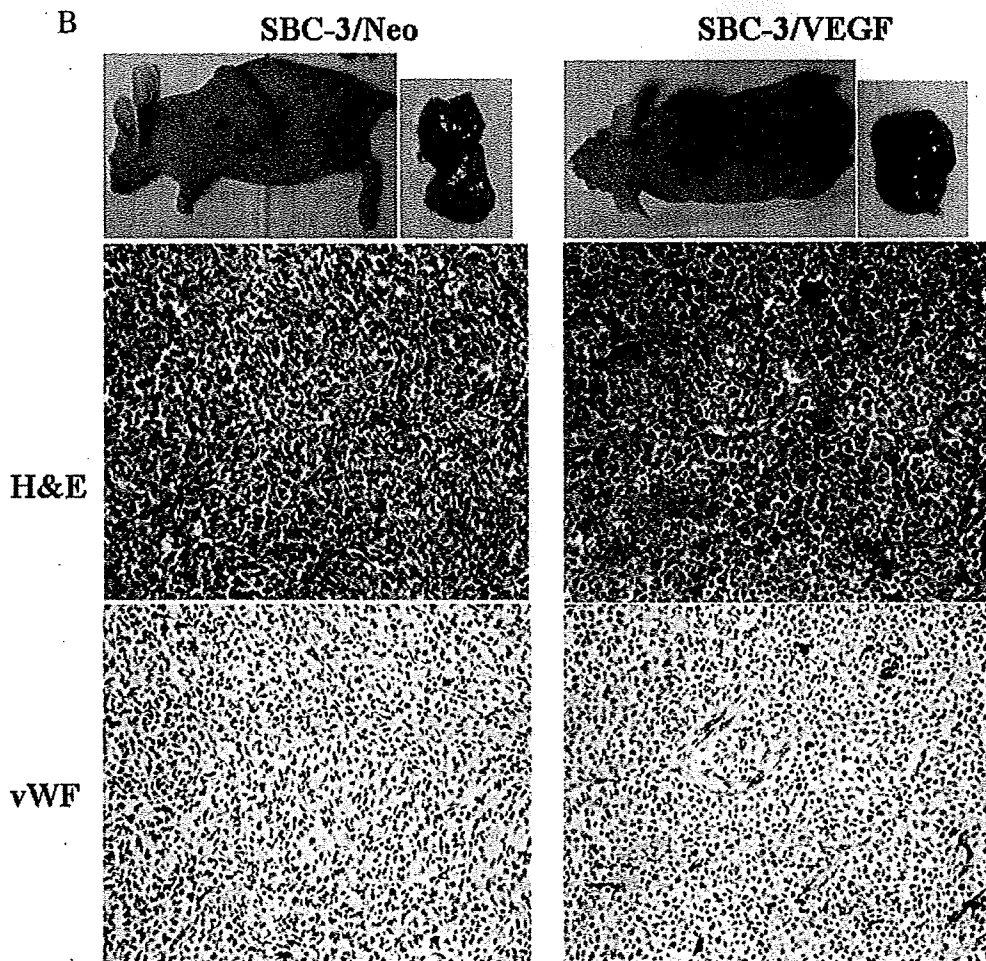
Table 3
Tumor-to-plasma concentration ratio (K_p) of analytes after an intravenous administration of NK012 (30 mg/kg) to nude mice bearing human colon cancer HT-29

Test article	Analyte		Time after administration (h)						
			0.0833	1	6	24	48	72	168
NK012	P-b SN-38*	Plasma ($\mu\text{g/mL}$)	612	410	254	23.3	1.25	0.278	0.0333
		Tumor ($\mu\text{g/g}$)	4.99	8.00	13.8	9.95	5.90	5.03	3.58
	P-u SN-38†	K_p (mL/g)‡	0.00815	0.0195	0.0543	0.427	4.72	18.1	108
		Plasma ($\mu\text{g/mL}$)	3.10	1.24	0.673	0.0717	0.0127	0.00925	0.00325
		Tumor ($\mu\text{g/g}$)	0.0763	0.187	0.188	0.0904	0.0531	0.0426	0.0358
		K_p (mL/g)‡	0.0246	0.151	0.279	1.26	4.18	4.61	11.0

NOTE: Data were expressed as means of three mice [56]. * Polymer-bound SN-38; SN-38 remaining bound to PEG-PGLu. † Polymer-unbound SN-38; free SN-38 from PEG-PGLu. ‡ K_p values were calculated on the mean concentrations of three mice.



cell line	SN-38	NK012	CPT-11
WiDR	0.046 ± 0.008	0.16 ± 0.014	20.4 ± 1.6
SW480	0.025 ± 0.003	0.11 ± 0.028	31.9 ± 1.3
Lovo	0.0067 ± 0.0012	0.026 ± 0.003	7.24 ± 1.04
HT-29	0.016 ± 0.003	0.068 ± 0.007	23.1 ± 2.63
PC-14	0.044 ± 0.025	0.14 ± 0.021	5.96 ± 0.90
SBC-3	0.0016 ± 0.001	0.0093 ± 0.005	0.72 ± 0.22
A431	0.0081 ± 0.002	0.019 ± 0.007	5.6 ± 1.5



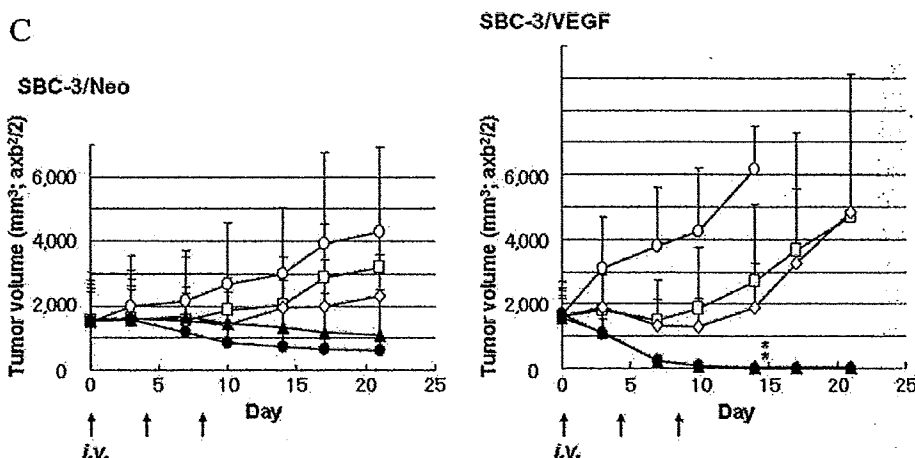


Fig. 14. Growth-inhibitory effect of NK012, SN-38, and CPT-11 on SBC-3/Neo and SBC-3/VEGF cells. (A) In *in vitro* experiment, the cells were exposed to the indicated concentrations of each drug for 72 h. The growth-inhibition curves and IC_{50} values for NK012 (▲), SN-38 (◆), and CPT-11 (■) are shown. (B) Representative photographs of massive tumors developed from SBC-3/Neo and SBC-3/VEGF at the time just before treatment initiation. Histological (H & E, $\times 20$) and Immunohistochemical (vWF, $\times 20$) examination for each tumor are shown. (C) Intravenous administration of NK012 or CPT-11 was started when the mean tumor volumes of groups reached a massive 1500 mm³. The mice were divided into test group (O: control; □: CPT-11 20 mg/kg/day; ◇: CPT-11 40 mg/kg/day; ▲: NK012 15 mg/kg/day; and ●: NK012 30 mg/kg/day). NK012 or CPT-11 was administered *i.v.* on days 0, 4, and 8. Each group consisted of 4 mice. * $P < 0.05$ [56].

fashion. On the other hand, NK012 (polymer-bound SN-38) exhibited slower clearance. The clearance of NK012 in the HT-29 tumor was significantly slower and the concentration of free

SN-38 was maintained at more than 30 ng/g even at 168 h after injection. The pharmacokinetic parameters of each drug in the plasma and tumor are depicted in Table 3.

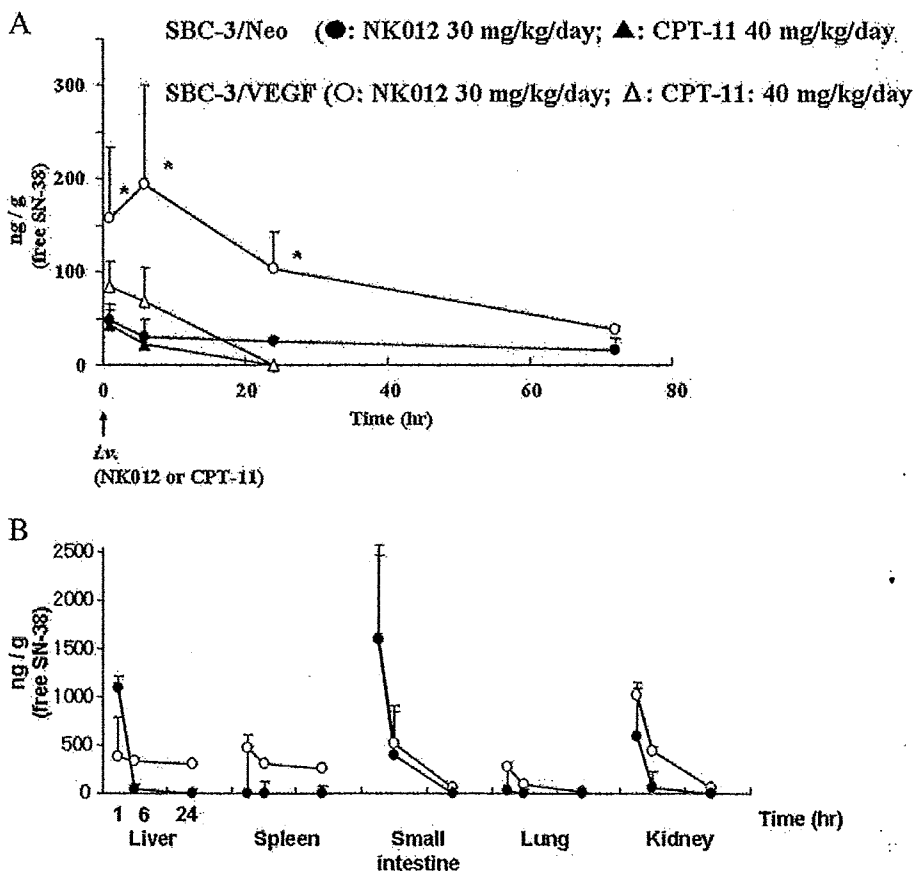


Fig. 15. Tissue and tumor distribution of free SN-38 after administration of NK012 and CPT-11. (A) Time profile of free SN-38 concentration in the SBC-3/Neo (●: NK012 30 mg/kg/day; ▲: CPT-11 40 mg/kg/day) and SBC-3/VEGF (O: NK012 30 mg/kg/day; Δ: CPT-11: 40 mg/kg/day). NK012 on day 0 and day 4 (96 h) or CPT-11 on day 0 were administered. * $P < 0.05$. (B) Tissue distribution of free SN-38 after single injection of NK012 at 30 mg/kg (O) and CPT-11 at 40 mg/kg (●) [56].

4.4. Anti-tumor activity and the distribution of NK012 and CPT-11 in SBC-3/Neo or SBC-3/VEGF tumors

In order to determine whether the potent antitumor effect of NK012 is enhanced in the tumors with high vascularity, we used vascular endothelial growth factor-secreting cells SBC-3/VEGF. There was no significant difference in the *in vitro* cytotoxic activity of each drug between SBC-3/Neo and SBC-3/VEGF (Fig. 14A). Gross findings of SBC-3/VEGF tumors are reddish as compared with SBC-3/Neo tumors (Fig. 14B). Deviating from the ordinary experimental tumor model, tumors were allowed to grow until they became massive in size, around 1.5 cm (Fig. 14C), and then the treatment was initiated. NK012 at doses of 15 and 30 mg/kg showed potent anti-tumor activity against bulky SBC-3/Neo tumors ($1533.1 \pm 1204.7 \text{ mm}^3$) as compared with CPT-11 (Fig. 14C). Striking antitumor activity was observed in mice treated with NK012 (Fig. 14C) when we compared the antitumor activity of NK012 with CPT-11 using SBC-3/VEGF cells. SBC-3/VEGF bulky masses ($1620.7 \pm 834.0 \text{ mm}^3$) disappeared in all mice, although relapse 3 months after treatment was noted in one mouse treated with NK012 20 mg/kg. On the other hand, SBC-3/VEGF were not eradicated and rapidly regrew after a partial response in mice treated with CPT-11. Approximate 10% body weight loss was observed in mice treated with NK012 20 mg/kg, but no significant difference was observed in comparison with mice treated with CPT-11 30 mg/kg.

We then examined the distribution of free SN-38 in the SBC-3/Neo and SBC-3/VEGF masses after administration of NK012 and CPT-11. In the case of CPT-11 administration, the concentrations at 1 and 6 h after the administration were less than 100 ng/g both in the SBC-3/Neo and SBC-3/VEGF tumors, and were almost negligible at 24 h in both tumors (Fig. 15A). There was no significant difference in the concentration between the SBC-3/Neo and SBC-3/VEGF tumors. On the other hand, in the case of NK012 administration, free SN-38 was detectable in the tumors even at 72 h after the administration. The concentrations of free SN-38 were higher in the SBC-3/VEGF tumors than those in the SBC-3/Neo tumors at any time point during the period of observation (significant at 1, 6, 24 h. $*P < 0.05$) (Fig. 15A).

4.5. Tissue distribution of SN-38 after administration of NK012 and CPT-11

We examined the concentration-time profile of free SN-38 in various tissues after *i.v.* administration of NK012 and CPT-11. All organs measured exhibited the highest concentration of SN-38 at 1 h after administration in mice given CPT-11 (Fig. 15B). On the other hand, mice given NK012 exhibited prolonged distribution in the liver and spleen (Fig. 15B). In a similar manner to other micellar drugs [39,53], NK012 demonstrated relatively higher accumulation in organs of the reticuloendothelial system. In the lung, kidney and small intestine, the highest concentration of free SN-38 was achieved at 1 h after injection of NK012 and the concentration was almost negligible at 24 h. Although the concentrations of free SN-38 in the small intestine were relatively high at 1 h after administration of NK012

and CPT-11, those rapidly decreased. Interestingly, there was no significant difference in the kinetic character of free SN-38 in the small intestine between mice treated with NK012 and CPT-11.

4.6. Synergistic antitumor activity of the NK012 combined with 5-fluorouracil

In two phase III trials, the addition of CPT-11 to bolus or infusional 5FU/LV regimens clearly yielded greater efficacy than treatment with 5FU/LV alone, with a doubling of the tumor response rate and prolongation of the median survival time by 2–3 months [54,55].

We demonstrated that the novel SN-38-incorporating polymeric micelles, NK012, exerted superior antitumor activity and less toxicity as compared to CPT-11 [53]. Therefore, we speculated that the use of NK012 in place of CPT-11 in combination with 5FU may also yield superior results.

4.6.1. Comparison of the antitumor effect of combined NK012/5FU and CPT-11/5FU

The therapeutic effect of CPT-11/5FU was apparently inferior to that of NK012/5FU or even NK012 alone at the MTD (Fig. 13). A more potent antitumor effect, namely 100% CR rate, was obtained in the NK012 alone and NK012/5FU groups, as compared with the 0% CR rate in the CPT-11/5FU [57].

4.6.2. Specificity of cell cycle perturbation

We studied the difference in the effects between NK012 and CPT-11 on the cell cycle. The data indicate that both NK012 and CPT-11 had a tendency to accumulate the cells in the S phase, although the effect of NK012 was stronger and maintained for a more prolonged period than that of CPT-11. The histograms show aneuploidy of the tumor and that administration of NK012 or CPT-11 caused apoptosis of a proportion of the tumor cells [57].

4.7. Present situation of a clinical study of NK012

A phase 1 study of NK012 is now under way in the National Cancer Center, Tokyo and Kashiwa in patients with advanced solid tumors. NK012 is infused intravenously over 60 min every 21 days until disease progression or unacceptable toxicity occurs.

5. Conclusion

A quarter of a century has passed since the EPR effect was discovered. Now the phrase EPR has become a fundamental principle in the field of DDS. Until recently, the EPR had not been recognized in the field of oncology. However, many oncologists have now become acquainted with it, since some drugs such as doxil, abraxane, and several PEGylated proteinaceous agents formulated based on the EPR have been approved in the field of oncology. Micelle carrier systems described in this chapter are obviously categorized as DDS based on the EPR. I believe that some anticancer agents incorporating micelle nanoparticles may be approved for clinical use soon.

Our next task is to develop DDS utilizing the EPR effect, which can accumulate selectively in solid tumors but also allow distribution of the delivered bullets (anticancer agents) through the entire mass of the solid tumor tissue.

References

- [1] Y. Matsumura, H. Maeda, A new concept for macromolecular therapeutics in cancer chemotherapy: mechanism of tumorotropic accumulation of proteins and the antitumor agent SMANCS, *Cancer Res.* 46 (1986) 6387–6392.
- [2] K. Kataoka, G.S. Kwon, M. Yokoyama, T. Okano, Y. Sakurai, Block copolymer micelles as vehicles for drug delivery, *J. Control. Release* 24 (1993) 119–132.
- [3] M. Yokoyama, M. Miyauchi, N. Yamada, T. Okano, Y. Sakurai, K. Kataoka, S. Inoue, Polymer micelles as novel drug carrier: adriamycin-conjugated poly(ethylene glycol)-poly(aspartic acid) block copolymer, *J. Control. Release* 11 (1990) 269–278.
- [4] M. Yokoyama, T. Okano, Y. Sakurai, H. Ekimoto, C. Shibazaki, K. Kataoka, Toxicity and antitumor activity against solid tumors of micelle-forming polymeric anticancer drug and its extremely long circulation in blood, *Cancer Res.* 51 (1991) 3229–3236.
- [5] D. Khayat, E.C. Antoine, D. Coeffic, Taxol in the management of cancers of the breast and the ovary, *Cancer Invest.* 18 (2000) 242–260.
- [6] D.N. Carney, Chemotherapy in the management of patients with inoperable non-small cell lung cancer, *Semin. Oncol.* 23 (1996) 71–75.
- [7] R.B. Weiss, R.C. Donehower, P.H. Wiernik, T. Ohnuma, R.J. Gralla, D.L. Trump, J.R. Baker Jr, D.A. Van Echo, D.D. Von Hoff, B. Leyland-Jones, Hypersensitivity reactions from taxol, *J. Clin. Oncol.* 8 (1990) 1263–1268.
- [8] E.K. Rowinsky, R.C. Donehower, Paclitaxel (taxol), *N. Engl. J. Med.* 332 (1995) 1004–1014;
R. Savic, L. Luo, A. Eisenberg, D. Maysinger, Micellar nanocontainers distribute to defined cytoplasmic organelles, *Science* 300 (2003) 615–618.
- [9] E.K. Rowinsky, V. Chaudhry, A.A. Forastiere, S.E. Sartorius, D.S. Ettinger, L.B. Grochow, B.G. Lubjeko, D.R. Cornblath, R.C. Donehower, Phase I and pharmacologic study of paclitaxel and cisplatin with granulocyte colony-stimulating factor: neuromuscular toxicity is dose-limiting, *J. Clin. Oncol.* 11 (1993) 2010–2020.
- [10] C. Wasserheit, A. Frazein, R. Oratz, J. Sorich, A. Downey, H. Hochster, A. Chachoua, J. Wernz, A. Zeleniuch-Jacquotte, R. Blum, J. Speyer, Phase II trial of paclitaxel and cisplatin in women with advanced breast cancer: an active regimen with limiting neurotoxicity, *J. Clin. Oncol.* 14 (1996) 1993–1999.
- [11] M. Yokoyama, T. Okano, Y. Sakurai, H. Ekimoto, C. Shibazaki, K. Kataoka, Toxicity and antitumor activity against solid tumors of micelle-forming polymeric anticancer drug and its extremely long circulation in blood, *Cancer Res.* 51 (1991) 3229–3236.
- [12] T. Hamaguchi, Y. Matsumura, M. Susuki, K. Shimizu, R. Goda, I. Nakamura, M. Nakatomi, K. Yokoyama, K. Kataoka, T. Kakizoe, NK105, a paclitaxel-incorporating micellar nanoparticle formulation, can extend in vivo antitumor activity and reduce the neurotoxicity of paclitaxel, *Br. J. Cancer* 92 (2005) 1240–1246.
- [13] R.B. Tishler, C.R. Geard, E.J. Hall, P.B. Schiff, Taxol sensitizes human astrocytoma cells to radiation, *Cancer Res.* 52 (1992) 3495–3497.
- [14] H. Choy, R.F. Devore 3rd, K.R. Hande, L.L. Porter, P. Rosenblatt, F. Yunus, L. Schlabach, C. Smith, Y. Shyr, D.H. Johnson, A phase II study of paclitaxel, carboplatin, and hyperfractionated radiation therapy for locally advanced inoperable non-small-cell lung cancer (a Vanderbilt Cancer Center Affiliate Network Study), *Int. J. Radiat. Oncol. Biol. Phys.* 47 (2000) 931–937.
- [15] M. Rodriguez, B.U. Sevin, J. Perras, H.N. Nguyen, C. Pham, A.J. Steren, O.R. Koechli, H.E. Averette, Paclitaxel: a radiation sensitizer of human cervical cancer cells, *Gynecol. Oncol.* 57 (1995) 165–169.
- [16] B.L. Lokeshwar, S.M. Ferrell, N.L. Block, Enhancement of radiation response of prostatic carcinoma by taxol: therapeutic potential for late-stage malignancy, *Anticancer Res.* 15 (1995) 93–98.
- [17] L. Milas, N.R. Hunter, K.A. Mason, B. Kurdoglu, L.J. Peters, Enhancement of tumor radioresponse of a murine mammary carcinoma by paclitaxel, *Cancer Res.* 54 (1994) 3506–3510.
- [18] L. Milas, N.R. Hunter, K.A. Mason, C.G. Milross, Y. Saito, L.J. Peters, Role of reoxygenation in induction of enhancement of tumor radioresponse by paclitaxel, *Cancer Res.* 55 (1995) 3564–3568.
- [19] A. Cividalli, G. Arcangeli, G. Cruciani, E. Livdi, E. Cordelli, D.T. Danesi, Enhancement of radiation response by paclitaxel in mice according to different treatment schedules, *Int. J. Radiat. Oncol. Biol. Phys.* 40 (1998) 1163–1170.
- [20] R.B. Tishler, C.R. Geard, E.J. Hall, P.B. Schiff, Taxol sensitizes human astrocytoma cells to radiation, *Cancer Res.* 52 (1992) 3495–3497.
- [21] A.G. Taghian, S.I. Assaad, A. Niemierko, I. Kuter, J. Younger, R. Schoenthaler, M. Roche, S.N. Powell, Risk of pneumonitis in breast cancer patients treated with radiation therapy and combination chemotherapy with paclitaxel, *J. Natl. Cancer Inst.* 93 (2001) 1806–1811.
- [22] H. Choy, W. Akerley, H. Safran, S. Graziano, C. Chung, T. Williams, B. Cole, T. Kennedy, Multiinstitutional phase II trial of paclitaxel, carboplatin, and concurrent radiation therapy for locally advanced non-small-cell lung cancer, *J. Clin. Oncol.* 16 (1998) 3316–3322.
- [23] J.E. Dowell, R. Sinard, D.A. Yardley, V. Aviles, M. Machtay, R.S. Weber, G.S. Weinstein, A.A. Chalian, D.P. Carbone, D.I. Rosenthal, Seven-week continuous-infusion paclitaxel concurrent with radiation therapy for locally advanced non-small cell lung and head and neck cancers, *Semin. Radiat. Oncol.* 9 (1999) 97–101.
- [24] D.P. Penney, P. Rubin, Specific early fine structural changes in the lung irradiation, *Int. J. Radiat. Oncol. Biol. Phys.* 2 (1977) 1123–1132.
- [25] P.A. Lind, L.B. Marks, P.H. Hardenbergh, R. Clough, M. Fan, D. Hollis, M.L. Hernandez, D. Lucas, A. Piepgrass, L.R. Prosnitz, Technical factors associated with radiation pneumonitis after local +/- regional radiation therapy for breast cancer, *Int. J. Radiat. Oncol. Biol. Phys.* 52 (2002) 137–143.
- [26] A.G. Taghian, S.I. Assaad, A. Niemierko, I. Kuter, J. Younger, R. Schoenthaler, M. Roche, S.N. Powell, Risk of pneumonitis in breast cancer patients treated with radiation therapy and combination chemotherapy with paclitaxel, *J. Natl. Cancer Inst.* 93 (2001) 1806–1811.
- [27] Y.M. Hanna, K.L. Baglan, J.S. Stromberg, F.A. Vicini, D. A Decker, Acute and subacute toxicity associated with concurrent adjuvant radiation therapy and paclitaxel in primary breast cancer therapy, *Breast J.* 8 (2002) 149–153.
- [28] T. Negishi, F. Koizumi, H. Uchino, J. Kuroda, T. Kawaguchi, S. Naito, Y. Matsumura, NK105, a paclitaxel-incorporating micellar nanoparticle, is a more potent radiosensitizing agent compared to free paclitaxel, *Br. J. Cancer* 95 (2006) 601–606.
- [29] T. Hamaguchi, K. Kato, H. Yasui, C. Morizane, M. Ikeda, H. Uchino, K. Muro, Y. Yamada, T. Okusaka, K. Shirao, Y. Yamada, H. Nakahama, Y. Matsumura, A phase I and pharmacokinetic study of NK105, a paclitaxel-incorporating micellar nanoparticle formulation, *Br. J. Cancer* 97 (2007) 170–176.
- [30] A. Horwich, D.T. Sleijfer, S.D. Fossa, S.B. Kaye, R.T. Oliver, M.H. Cullen, G.M. Mead, R. de Wit, P.H. de Mulder, D.P. Dearnaley, P.A. Cook, R.J. Sylvester, S.P. Stenning, Randomized trial of bleomycin, etoposide, and cisplatin compared with bleomycin, etoposide, and carboplatin in good-prognosis metastatic nonseminomatous germ cell cancer: a Multiinstitutional Medical Research Council/European Organization for Research and Treatment of Cancer Trial, *J. Clin. Oncol.* 15 (1997) 1844–1852.
- [31] B.J. Roth, Chemotherapy for advanced bladder cancer, *Semin. Oncol.* 23 (1996) 633–644;
D. Screnci, M.J. McKeage, P. Galetti, T.W. Hambley, B.D. Palmer, B.C. Baguley, Relationships between hydrophobicity, reactivity, accumulation and peripheral nerve toxicity of a series of platinum drugs, *Br. J. Cancer.* 82 (2000) 966–972.
- [32] V. Pinzani, F. Bressolle, I.J. Haug, M. Galtier, J.P. Blayac, P. Balmes, Cisplatin-induced renal toxicity and toxicity-modulating strategies: a review, *Cancer Chemother. Pharmacol.* 35 (1994) 1–9.
- [33] M.J. Cleare, P.C. Hydes, B.W. Malerbi, D.M. Watkins, Anti-tumor platinum complexes: relationships between chemical properties and activity, *Biochimie* 60 (1978) 835–850.

- [34] A. du Bois, H.J. Luck, W. Meier, H.P. Adams, V. Mobus, S. Costa, T. Bauknecht, B. Richter, M. Warm, W. Schroder, S. Olbricht, U. Nitz, C. Jackisch, G. Emons, U. Wagner, W. Kuhn, J. Pfisterer, A randomized clinical trial of cisplatin/paclitaxel versus carboplatin/paclitaxel as first-line treatment of ovarian cancer, *J. Natl. Cancer Inst.* 95 (2003) 1320–1329.
- [35] J. Cassidy, J. Taberero, C. Twelves, R. Brunet, C. Butts, T. Conroy, F. Debraud, A. Figer, J. Grossmann, N. Sawada, P. Schoffski, A. Sobrero, E. Van Cutsem, E. Diaz-Rubio, XELOX (capecitabine plus oxaliplatin): active first-line therapy for patients with metastatic colorectal cancer, *J. Clin. Oncol.* 22 (2004) 2084–2091.
- [36] A. Horwich, D.T. Sleijfer, S.D. Fossa, S.B. Kaye, R.T. Oliver, M.H. Cullen, G.M. Mead, R. de Wit, P.H. de Mulder, D.P. Deamaley, P.A. Cook, R.J. Sylvester, S.P. Stenning, Randomized trial of bleomycin, etoposide, and cisplatin compared with bleomycin, etoposide, and carboplatin in good-prognosis metastatic nonseminomatous germ cell cancer: a Multiinstitutional Medical Research Council/European Organization for Research and Treatment of Cancer Trial, *J. Clin. Oncol.* 15 (1997) 1844–1852.
- [37] J. Bellmunt, A. Ribas, N. Eres, J. Albanell, C. Almanza, B. Bermejo, L.A. Sole, J. Baselga, Carboplatin-based versus cisplatin-based chemotherapy in the treatment of surgically incurable advanced bladder carcinoma, *Cancer* 80 (1997) 1966–1972.
- [38] N. Nishiyama, S. Okazaki, H. Cabral, M. Miyamoto, Y. Kato, Y. Sugiyama, K. Nishio, Y. Matsumura, K. Kataoka, Novel cisplatin-incorporated polymeric micelles can eradicate solid tumors in mice, *Cancer Res.* 63 (2003) 8977–8983.
- [39] H. Uchino, Y. Matsumura, T. Negishi, F. Koizumi, T. Hayashi, T. Honda, et al., Cisplatin-incorporating polymeric micelles (NC-6004) can reduce nephrotoxicity and neurotoxicity of cisplatin in rats, *Br. J. Cancer* 93 (2005) 678–687.
- [40] L.H. Li, T.J. Fraser, E.J. Olin, B.K. Bhuyan, Action of camptothecin on mammalian cells in culture, *Cancer Res.* 32 (1972) 2643–2650.
- [41] R.C. Gallo, J. Whang-Peng, R.H. Adamson, Studies on the antitumor activity, mechanism of action, and cell cycle effects of camptothecin, *J. Natl. Cancer Inst.* 46 (1971) 789–795.
- [42] J.A. Gottlieb, A.M. Guarino, J.B. Call, V.T. Oliverio, J.B. Block, Preliminary pharmacologic and clinical evaluation of camptothecin sodium (NSC-100880), *Cancer Chemother. Rep.* 54 (1970) 461–470.
- [43] F.M. Muggia, P.J. Creaven, H.H. Hansen, M.H. Cohen, O.S. Selawry, Phase I clinical trial of weekly and daily treatment with camptothecin (NSC-100880): correlation with preclinical studies, *Cancer Chemother. Rep.* 56 (1972) 515–521.
- [44] D. Cunningham, S. Pyrhonen, R.D. James, C.J. Punt, T.F. Hickish, R. Heikkila, et al., Randomised trial of irinotecan plus supportive care versus supportive care alone after fluorouracil failure for patients with metastatic colorectal cancer, *Lancet* 352 (1998) 1413–1418.
- [45] L.B. Saltz, J.V. Cox, C. Blanke, L.S. Rosen, L. Fehrenbacher, M.J. Moore, et al., Irinotecan plus fluorouracil and leucovorin for metastatic colorectal cancer. Irinotecan Study Group, *N. Engl. J. Med.* 343 (2000) 905–914.
- [46] K. Noda, Y. Nishiwaki, M. Kawahara, S. Negoro, T. Sugiura, A. Yokoyama, et al., Irinotecan plus cisplatin compared with etoposide plus cisplatin for extensive small-cell lung cancer, *N. Engl. J. Med.* 346 (2002) 85–91.
- [47] S. Negoro, N. Masuda, Y. Takada, T. Sugiura, S. Kudoh, N. Katakami, et al., CPT-11 Lung Cancer Study Group West. Randomised phase III trial of irinotecan combined with cisplatin for advanced non-small-cell lung cancer, *Br. J. Cancer* 88 (2003) 335–341.
- [48] D.C. Bodurka, C. Levenback, J.K. Wolf, J. Gano, J.T. Wharton, J.J. Kavanagh, et al., Phase II trial of irinotecan in patients with metastatic epithelial ovarian cancer or peritoneal cancer, *J. Clin. Oncol.* 21 (2003) 291–297.
- [49] C.H. Takimoto, S.G. Arbuck, Topoisomerase I targeting agents: the camptothecins, in: B.A. Chabner, D.L. Lango (Eds.), *Cancer Chemotherapy and Biotherapy: Principal and Practice*, 3rd ed., Lippincott Williams & Wilkins, Philadelphia (PA), 2001, pp. 579–646.
- [50] J.G. Slatter, L.J. Schaaf, J.P. Sams, K.L. Feenstra, M.G. Johnson, P.A. Bombardt, et al., Pharmacokinetics, metabolism, and excretion of irinotecan (CPT-11) following I.V. infusion of [(14)C]CPT-11 in cancer patients, *Drug Metab. Dispos.* 28 (2000) 423–433.
- [51] M.L. Rothenberg, J.G. Kuhn, H.A. Burrell 3rd, J. Nelson, J.R. Eckardt, M. Tristan-Morales, et al., Phase I and pharmacokinetic trial of weekly CPT-11, *J. Clin. Oncol.* 11 (1993) 2194–2204.
- [52] S. Guichard, C. Terret, I. Hennebelle, I. Lochon, P. Chevreau, E. Fretigny, et al., CPT-11 converting carboxylesterase and topoisomerase activities in tumor and normal colon and liver tissues, *Br. J. Cancer* 80 (1999) 364–370.
- [53] M. Yokoyama, T. Okano, Y. Sakurai, H. Ekimoto, C. Shibasaki, K. Kataoka, Toxicity and antitumor activity against solid tumors of micelle-forming polymeric anticancer drug and its extremely long circulation in blood, *Cancer Res.* 51 (1991) 3229–3236.
- [54] L.B. Saltz, J.Y. Douillard, N. Pirota, et al., Irinotecan plus fluorouracil/leucovorin for metastatic colorectal cancer: a new survival standard, *Oncologist* 6 (2001) 81–91.
- [55] J.Y. Douillard, D. Cunningham, A.D. Roth, et al., Irinotecan combined with fluorouracil compared with fluorouracil alone as first-line treatment for metastatic colorectal cancer: a multicentre randomised trial, *Lancet* 355 (2000) 1041–1047.
- [56] F. Koizumi, M. Kitagawa, T. Negishi, et al., Novel SN-38-incorporating polymeric micelles, NK012, eradicate vascular endothelial growth factor-secreting bulky tumors, *Cancer Res.* 66 (2006) 10048–10056.
- [57] T. Eguchi Nakajima, M. Yasunaga, Y. Kano, K. Shirao, Y. Shimada, Y. Matsumura, Synergistic antitumor activity of the novel SN-38-incorporating polymeric micelles, NK012, combined with 5-fluorouracil in a mouse model of colorectal cancer, as compared with that of irinotecan plus 5-fluorouracil, *Int. J. Cancer.* 122 (2008) 2148–2153.

Antitumor Effect of SN-38–Releasing Polymeric Micelles, NK012, on Spontaneous Peritoneal Metastases from Orthotopic Gastric Cancer in Mice Compared with Irinotecan

Takako Eguchi Nakajima,^{1,2} Kazuyoshi Yanagihara,³ Misato Takigahira,³ Masahiro Yasunaga,¹ Ken Kato,² Tetsuya Hamaguchi,² Yasuhide Yamada,² Yasuhiro Shimada,² Keichiro Mihara,⁵ Takahiro Ochiya,⁴ and Yasuhiro Matsumura¹

¹Investigative Treatment Division, Research Center for Innovative Oncology, National Cancer Center Hospital East, Kashiwa, Chiba, Japan; ²Gastrointestinal Oncology Division, National Cancer Center Hospital, ³Central Animal Laboratory, and ⁴Section for Studies on Metastasis, National Cancer Center Research Institute, Tokyo, Japan; and ⁵Hematology and Oncology Department, Clinical and Experimental Oncology Division, Research Institute for Radiation Biology and Medicine, Hiroshima University, Hiroshima, Japan

Abstract

7-Ethyl-10-hydroxy-camptothecin (SN-38), an active metabolite of irinotecan hydrochloride (CPT-11), has potent antitumor activity. Moreover, we have reported the strong antitumor activity of NK012 (i.e., SN-38–releasing polymeric micelles) against human cancer xenografts compared with CPT-11. Here, we investigated the advantages of NK012 over CPT-11 treatment in mouse models of gastric cancer with peritoneal dissemination. NK012 or CPT-11 was i.v. administered thrice every 4 days at their respective maximum tolerable doses (NK012, 30 mg/kg/day; CPT-11, 67 mg/kg/day) to mice receiving orthotopic transplants of gastric cancer cell lines (44As3Luc and 58As1mLuc) transfected with the luciferase gene ($n = 5$). Antitumor effect was evaluated using the photon counting technique. SN-38 concentration in gastric tumors and peritoneal nodules was examined by high-performance liquid chromatography (HPLC) 1, 24, and 72 hours after each drug injection. NK012 or CPT-11 distribution in these tumors was evaluated using a fluorescence microscope on the same schedule. In both models, the antitumor activity of NK012 was superior to that of CPT-11. High concentrations of SN-38 released from NK012 were detected in gastric tumors and peritoneal nodules up to 72 hours by HPLC. Only a slight conversion from CPT-11 to SN-38 was observed from 1 to 24 hours. Fluorescence originating from NK012 was detected up to 72 hours, whereas that from CPT-11 disappeared until 24 hours. NK012 also showed antitumor activity against peritoneal nodules. Thus, NK012 showing enhanced distribution with prolonged SN-38 release may be ideal for cancer treatment because the antitumor activity of SN-38 is time dependent. [Cancer Res 2008;68(22):9318–22]

Introduction

Gastric cancer is the second most common cause of death from cancer in the world. The survival rate has remained low in patients with advanced gastric cancer, with a median survival rate of 13 months having been recently reported in a phase III trial, which

has been the best outcome thus far (1). Patients with gastric cancer with scirrhous type stroma particularly showed poor prognosis even after curative resection, as well as highly progressed peritoneal dissemination (2). Because peritoneal dissemination causes several refractory symptoms such as massive ascites, intestinal obstruction, hydronephrosis, and obstructive jaundice, the quality of life of patients at the end stage of cancer is severely impaired.

Poor delivery of anticancer drugs to peritoneal metastatic cells may be one of the reasons for the poor prognosis of patients with peritoneal dissemination (3). In peritoneal nodules, the distribution and eventual diffusion of drugs to cancer cells tend to be impeded because of several obstacles such as severe fibrosis and high interstitial pressure (4, 5). On the other hand, angiogenesis was reported to be an essential factor in the development of peritoneal metastasis, and the high expression level of vascular endothelial growth factor (VEGF) in primary gastric tumors or ascitic fluid, which can enhance tumor vascular permeability, was found to be directly associated with the development of ascites and peritoneal dissemination (6–10). In addition, several factors such as kinins and nitric oxide are involved in tumor vascular permeability (11–13). Polymer-conjugated drugs and nanoparticles categorized under drug delivery system agents are favorably extravasated from the vessels into the interstitium of tumors due to the enhanced permeability and retention effect (EPR effect; refs. 14, 15). The EPR effect is based on the following pathophysiologic characteristics of solid tumor tissues: hypervascularity, incomplete vascular architecture, secretion of vascular permeability factors stimulating extravasation within cancer tissue, and absence of effective lymphatic drainage from the tumors that impedes the efficient clearance of macromolecules accumulated in solid tumor tissues. Moreover, macromolecules cannot freely leak out from normal vessels, and thus, the side effects of an anticancer agent can be reduced. Very recently, we have shown that NK012 (i.e., SN-38–releasing polymeric micelles) exerted superior antitumor activity and less toxicity than CPT-11 (15–17). In a series of studies, we showed that NK012 markedly enhanced the antitumor activity of SN-38, particularly against highly VEGF-secreting SBC-3/VEGF tumors compared with SBC-3/Neo tumors. On the other hand, it is conceivable that satisfactory drug delivery cannot be achieved in less-vascularized and highly fibrotic tumors, particularly for macromolecules. However, we observed that NK012 showed a strong antitumor activity even in the xenograft of Capan1 cells, which are pancreatic cancer cells with abundant stromal tissue, compared with CPT-11. This result suggests that NK012 can selectively accumulate in both hypervascular and hypovascular tumors with high interstitial pressure, and then induce sustained

Requests for reprints: Yasuhiro Matsumura, Investigative Treatment Division, Research Center for Innovative Oncology, National Cancer Center Hospital East, 6-5-1 Kashiwanoha, Kashiwa, Chiba 277-8577, Japan. Phone: 81-4-7134-6857; Fax: 81-4-7134-6866; E-mail: ymatsum@east.ncc.go.jp.

©2008 American Association for Cancer Research.
doi:10.1158/0008-5472.CAN-08-2822

release of SN-38, followed by SN-38 distribution throughout the entire tumor tissues. In the present study, we evaluated the antitumor activity of NK012 against peritoneal tumor dissemination compared with that of CPT-11 using mouse models orthotopically transplanted with scirrhous gastric cancer cells, as well as against spontaneously progressing peritoneal dissemination (18, 19).

Materials and Methods

Cell cultures. 44As3 and 58As1m were previously reported as human signet-ring cell gastric cancer cell lines that spontaneously metastasize to the peritoneal cavity and produce large volumes of bloody ascites after orthotopic implantation in the gastric wall (18–21). Here, 44As3 and 58As1m cells were transfected with a complex of 4 μ g of pEGF-PLuc plasmid DNA (Clontech) and 24 μ L of GeneJammer reagent (Stratagene; Cloning Systems) in accordance with the manufacturer's instructions. Stable transfectants were selected in geneticin (400 μ g/mL; Invitrogen), and bioluminescence was used to screen transfected clones for luciferase gene expression using the IVIS system (Xenogen). Clones expressing the luciferase gene were named 44As3Luc and 58As1mLuc. 44As3Luc and 58As1mLuc cells were maintained in RPMI 1640 supplemented with 10% FCS (Sigma), 100 IU/mL penicillin G sodium, and 100 mg/mL streptomycin sulfate (Immuno-Biological Laboratories) in a humidified atmosphere containing 5% CO₂ at 37°C.

Orthotopic models *in vivo*. Six-week-old female BALB/c *nu/nu* mice were purchased from CLEA Japan, Inc., and maintained under specific pathogen-free conditions and provided with sterile food, water, and cages. Ambient light was controlled to provide regular cycles of 12 h of light and 12 h of darkness. A total of 1×10^6 cells of 44As3Luc or 58As1mLuc were inoculated into the gastric wall of each mouse after laparotomy, as described previously (18–21). *In vivo* photon counting analysis was conducted on a cryogenically cooled IVIS system using Living Image acquisition and analysis software (Xenogen). All animal procedures were performed in compliance with the Guidelines for the Care and Use of

Experimental Animals established by the Committee for Animal Experimentation of the National Cancer Center; these guidelines conform to the ethical standards required by law and also comply with the guidelines for the use of experimental animals in Japan.

Drugs. NK012 was prepared by Nippon Kayaku Co., Ltd. (15). CPT-11 was purchased from Yakult Honsha Co., Ltd.

***In vivo* growth inhibition assay.** After inoculation of 44As3Luc or 58As1mLuc cells into the gastric wall (day 0), mice were randomly divided into test groups consisting of 5 mice per group. 44As3Luc mice were *i.v.* administered the maximum tolerated dose (MTD) of the 2 drugs via the tail vein on days 20, 24, and 28 as previously reported, that is, at 66.7 mg/kg/d for CPT-11 and 30 mg/kg/d for NK012 (15). 58As1mLuc mice were given the drugs in the same manner on days 18, 22, and 26. Photon counting analysis and body weight were measured twice a week. "Visible ascites," which was evident a few days before death in this mouse model, was used as a surrogate for survival time in consideration of animal welfare. Mice were euthanized when ascites became visible, and colonization of gastric wall by cancer cells and metastasis to the peritoneal cavity were confirmed in all the euthanized mice. Differences in relative photon counts between the treatment groups at day 42 in 44As3Luc mice and at day 81 in 58As1mLuc mice were analyzed using the unpaired *t* test.

Assay of free SN-38 in tissues. We next analyzed the biodistributions of NK012 and CPT-11 to orthotopic gastric tumors and peritoneal nodules. Twenty-six days after the inoculation of 44As3Luc cells into the gastric wall of mice, NK012 (30 mg/kg) or CPT-11 (66.7 mg/kg) was administered via the tail vein. Under anesthesia, orthotopic gastric tumor and peritoneal nodule samples were excised 1, 24, and 72 hours after injection.

Measurements of tissue concentration of free SN-38 by high-performance liquid chromatography. Samples were rinsed with physiologic saline, mixed with 0.1 mol/L glycine-HCl buffer (pH 3.0)/methanol at 5 w/w%, and then homogenized. To analyze the concentration of free SN-38, 100 μ L of the tumor samples were mixed with 20 μ L of 1 mmol/L phosphoric acid/methanol (1:1) and 40 μ L of ultrapure water, and camptothecin (CPT) was used as the internal standard (10 ng/mL for free SN-38). The samples were vortexed vigorously for 10 s, and then filtered

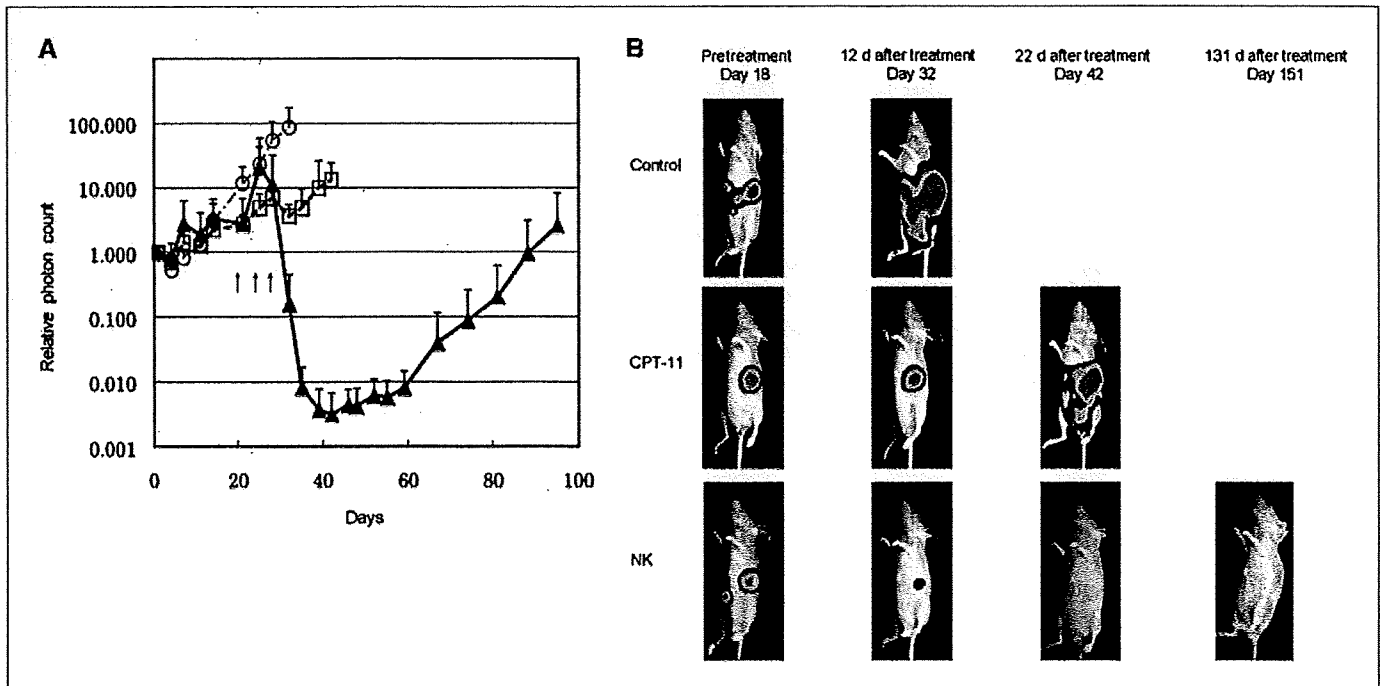


Figure 1. Effects of NK012 and CPT-11 in 44As3Luc mouse models. *A*, antitumor activity of NK012 or CPT-11 was evaluated by counting the number of photons using the IVIS system (points, mean; bars, SD; arrows, drug injections). Antitumor effect of each regimen on days 20, 24, and 28. (○), control; (□), CPT-11 (66.7 mg/kg/d, $\times 3$); and (▲), NK012 (30 mg/kg/d, $\times 3$) in 44As3Luc mouse model. *B*, images of 44As3Luc mouse model administered NK012 taken using the IVIS system on days 18, 32, 42, and 151 after inoculation of 44As3Luc cells. Data were derived from the same mice as those used in the present study.

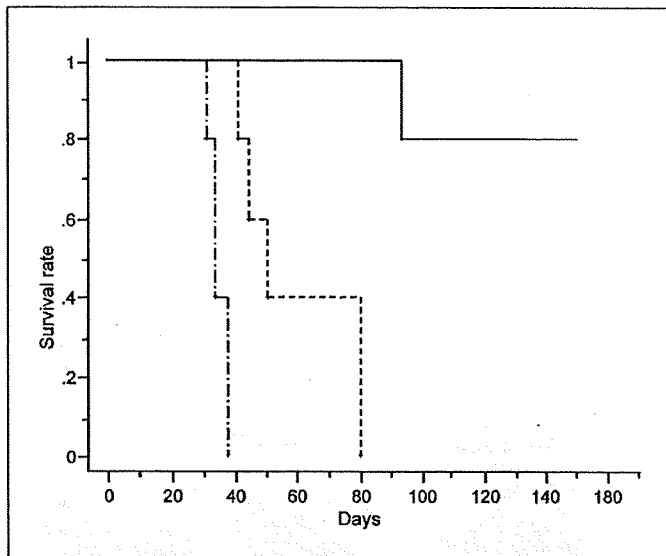


Figure 2. Survival curves of 44As3Luc mouse models. Survival curves of 44As3Luc mouse model in each regimen on days 20, 24, and 28. (— · — ·), control; (---), CPT-11 given at 66.7 mg/kg/d \times 3; and (—), NK012 given at 30 mg/kg/d \times 3.

through Ultrafree-MC Centrifugal Filter Devices with a cutoff molecular diameter of 0.45 μ m (Millipore Co.). Reversed-phase high-performance liquid chromatography (HPLC) was conducted at 35°C on a Mightysil RP-18 GP column (150 \times 4.6 mm; Kanto Chemical Co., Inc.). Fifty microliters of a sample were injected into an Alliance Water 2795 HPLC system (Waters) equipped with a Waters 2475 multi λ fluorescence detector. Fluorescence originating from SN-38 was detected at 540 nm with an excitation wavelength of 365 nm. The mobile phase was a mixture of 100 mmol/l ammonium acetate (pH 4.2) and methanol [11:9 (v/v)], and the flow rate was 1.0 mL/min. The content of SN-38 was calculated by measuring the relevant peak area and calibrating against the corresponding peak area derived from the CPT internal standard. Peak data were recorded using a chromatography management system (MassLynx v4.0; Waters).

Visualization of distribution of NK012 and CPT-11 by fluorescence microscopy. Mice were given fluorescein *Lycopersicon esculentum* lectin (100 μ L per mouse; Vector Laboratories) to visualize tumor vasculature in the samples 5 min before anesthesia. The samples were then excised and embedded in an optimal cutting temperature compound (Sakura Finetechnochemical Co., Ltd.) and frozen at -80° C. Six- μ m-thick tumor sections were then prepared using a cryostatic microtome, Tissue-Tek Cryo3 (Sakura Finetechnochemical Co., Ltd.). Frozen sections were examined under a fluorescence microscope, BIOZERO (KEYENCE), at an excitation wavelength of 377 nm and an emission wavelength 447 nm to evaluate the distribution of NK012 and CPT-11. Both drugs could be detected under the same fluorescence conditions because formulations containing SN-38 bound via ester bonds possess a particular fluorescence.

Statistical analyses. Data were expressed as mean \pm SD. Data were analyzed using the Student's *t* test when groups showed equal variances (*F* test), or the Welch's test when they showed unequal variances (*F* test). *P* value of <0.05 was considered as significant. All statistical tests were two sided.

Results

Antitumor activities of NK012 and CPT-11. Comparison of the relative photon counts on day 42 in the 44As3Luc mouse model revealed significant differences in counts between mice given with NK012 and those given with CPT-11 (*P* = 0.0282; Fig. 1A and B).

Similar result was obtained in the experiment with 58As gastric tumor (data not shown). The survival rates on day 150 in the 44As3Luc mouse model were 80% and 0% for the NK012 group and CPT-11 group, respectively (Fig. 2). Similar result was obtained in the experiment with 58As gastric tumor (data not shown). No marked toxic effects in terms of body weight changes were observed in any groups for any mouse models (data not shown). Only 1 mouse in the CPT-11 group of 44As1 mouse models showed diarrhea for 3 d, and any other clinical symptoms were not observed.

Tissue concentrations of free SN-38 after administration of NK012 and CPT-11. We examined the concentration-time profile of free SN-38 in orthotopic gastric tumors and peritoneal nodules in the 44As3Luc mouse model after the administration of NK012 and CPT-11 (Fig. 3A and B). Either orthotopic gastric tumors or peritoneal nodules exhibited the highest concentration of free SN-38 24 hours after NK012 administration, and 1 hour after CPT-11 administration. The highest concentrations of free SN-38 in the NK012 group were much higher than those in the CPT-11 group in either orthotopic gastric tumors or peritoneal nodules. The concentrations of free SN-38 released from NK012 in orthotopic gastric tumors were higher than those in peritoneal nodules.

Tumor tissue distribution of NK012 and CPT-11 as determined by fluorescence microscopy. Results showed that NK012 accumulation in either orthotopic gastric tumors or peritoneal nodules had been maintained from 1 hour to 72 hours after injection (Fig. 4A). On the other hand, CPT-11 showed maximum accumulation in either orthotopic gastric tumors or peritoneal nodules 1 hour after injection and disappeared within 24 hours (Fig. 4B).

Discussion

The main purpose of this study was to clarify the advantages of NK012 over CPT-11 as treatment against peritoneal metastasis spontaneously disseminated from orthotopically transplanted scirrhous gastric cancer cells in mouse models. We showed that NK012 exerted more potent antitumor activity in the mouse models used than CPT-11. Therefore, NK012 is considered promising in terms of providing clinical benefit to patients with gastric cancer showing progressing peritoneal dissemination.

CPT-11 is converted to SN-38, a biologically active and water-insoluble metabolite of CPT-11, by carboxylesterases (CE) in the liver and tumors. However, only 2% to 8% of administered CPT-11 is converted by CE in the liver and tumors to the active form SN-38 (22, 23). The conversion of CPT-11 to SN-38 also depends on genetic interindividual variability of the activity of CE (24). Thus, the direct use of SN-38 might be of great advantage and is attractive for cancer treatment. We have recently shown that NK012 (i.e., SN-38-releasing polymeric micelles) exerted superior antitumor activity and less toxicity than CPT-11 (15–17). The mean particle size of NK012 is 20 nm in diameter. NK012 can release SN-38 under neutral conditions even in the absence of CE because SN-38, which is bound to the blockcopolymer by phenolic ester binding, is stable under acidic conditions but relatively labile under neutral and mild alkaline conditions. The release rate of SN-38 from NK012 under physiologic conditions is quite high, that is, $>70\%$ of SN-38 is gradually released within 48 hours.

In this study, we used mouse models with orthotopically transplanted human scirrhous gastric cancer cells showing spontaneously progressing peritoneal dissemination, which we

reported previously (18, 19, 21). These models can imitate more realistically the progressing mode of human peritoneal dissemination of gastric cancer than conventional experimental models directly transplanted with cancer cells *i.p.* Moreover, our models enabled us to quantitatively evaluate drug antitumor effect even against peritoneal dissemination without having to sacrifice the animal and perform autopsy through the use of gastric cancer cells transfected with the luciferase gene and by applying photon counting analysis, having already verified the significant correlation between tumor volume and photon counts in a previous report (19).

For *in vivo* growth inhibition assay, drug administration was started on day 18 or 20 after cell inoculation into the gastric wall, when small peritoneal metastatic nodules and a small degree of ascites had appeared. The present results showed that NK012 had more potent antitumor activity than CPT-11 in the mouse models tested, suggesting its effectiveness against peritoneal dissemination of gastric cancer in the clinical setting.

In the pharmacologic evaluation, we could confirm the more enhanced distribution of NK012 than CPT-11 to not only orthotopic gastric tumors but also peritoneal nodules by quantifying SN-38 concentration in the tumors and visualization of fluorescence originating from NK012 or CPT-11 distributed in the tumors. Because CPT-11 or SN-38 has been reported to possess time-dependent growth-inhibitory activity against tumor cells, this prolonged retention of NK012 in the tumors and the sustained release of free SN-38 from NK012 may be responsible for its more potent antitumor activity observed in the present study (25). On the other hand, CPT-11 disappeared from the tumors before exerting sufficient antitumor activity. For both drugs, however, the concentrations of SN-38 in orthotopic gastric tumors were higher than those

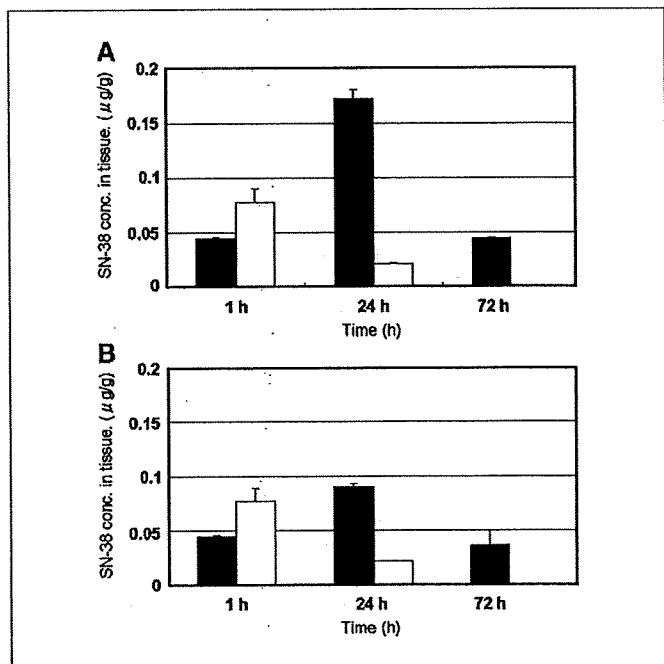


Figure 3. Concentration-time profile of free SN-38. NK012 (30 mg/kg) or CPT-11 (66.7 mg/kg) was injected 26 d after implantation of 44As3Luc gastric cancer cells (columns, mean; bars, SD). *A*, concentration (conc.) of free SN-38 in orthotopic gastric tumor tissue of 44As3Luc mouse model after administration of NK012 (black column) and CPT-11 (white column). *B*, concentration of free SN-38 in peritoneal nodules of 44As3Luc mouse model after administration of NK012 (black column) and CPT-11 (white column).

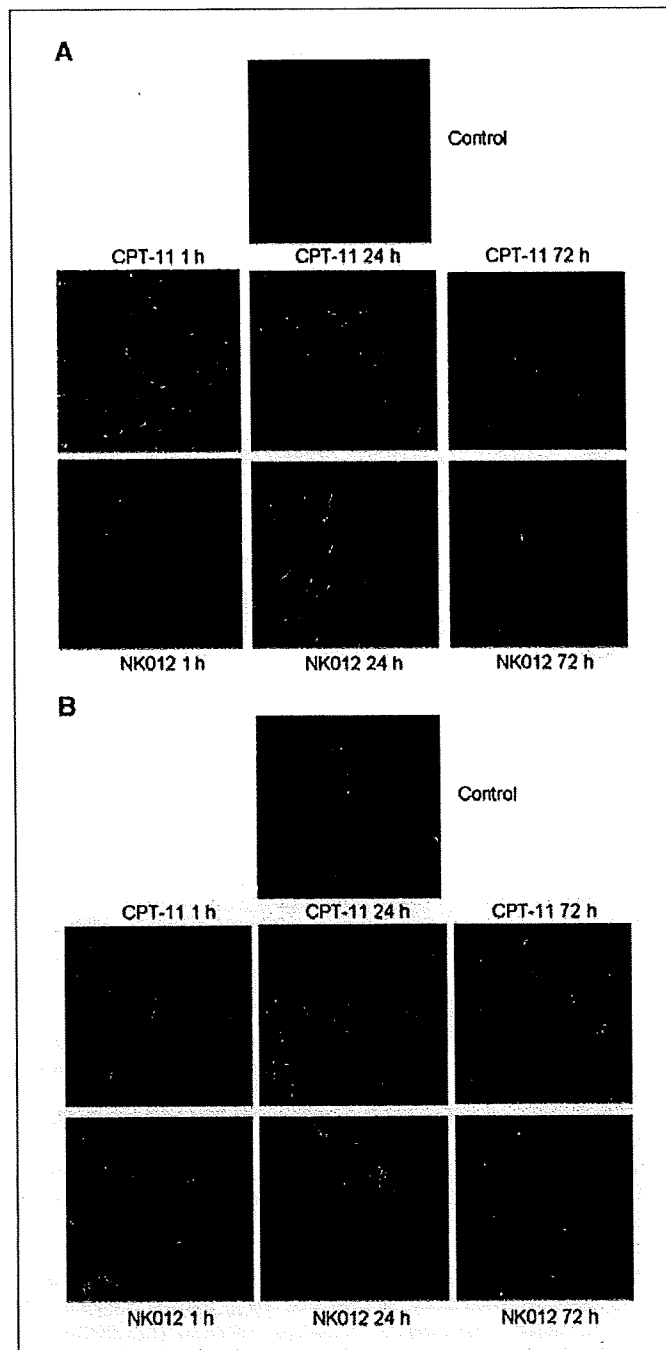


Figure 4. Tissue distribution of NK012 and CPT-11 as determined by fluorescence microscopy. Orthotopic gastric tumors or peritoneal nodules of 44As3Luc mouse model were excised 1, 24, and 72 h after *i.v.* injection of NK012 (30 mg/kg) or CPT-11 (66.7 mg/kg). Each mouse was *i.v.* administered with fluorescein-labeled *Lycopersicon esculentum* lectin just before being sacrificed to detect tumor blood vessels. Frozen sections were examined under a fluorescence microscope at an excitation wavelength of 377 nm and an emission wavelength of 447 nm. The same fluorescence condition can be applied for visualizing NK012 and CPT-11 fluorescence. Free SN-38 cannot be detected under this fluorescence condition. *A*, distribution of NK012 or CPT-11 in orthotopic gastric tumors ($\times 100$). *B*, distribution of NK012 or CPT-11 in peritoneal nodules ($\times 100$).

in peritoneal nodules. This is consistent with previous reports stating the poor delivery of anticancer drugs to peritoneal metastatic cells probably because of some obstacles such as abundant interstitium or high interstitial pressure. To date, we reported that NK012 can

more selectively accumulate and retain longer in various tumor xenografts transplanted s.c. compared with CPT-11 (15–17). In the present study, we succeeded in demonstrating higher accumulation and longer retention of NK012 compared with CPT-11 in orthotopic and peritoneal disseminated gastric cancer model that is closer to human gastric cancer in clinics.

Peritoneal dissemination sometimes causes intestinal obstruction, which enhances the enterohepatic circulation of SN-38 after direct damage to the small intestine, and makes the use of CPT-11 difficult (26, 27). In the present study, no mouse in the NK012 group developed diarrhea. The dose-limiting toxic effects of CPT-11 seem to be neutropenia and diarrhea. In our previous data, however, there was no significant difference in the level of SN-38 in the small intestine between mice treated with NK012 and mice treated with CPT-11 despite the higher plasma area under the concentration of NK012 than CPT-11 (15). Moreover, no serious diarrhea has been reported even at the MTD dose in two phase I clinical trials against advanced solid tumors in Japan and the US (28, 29).

In conclusion, we showed that NK012 exerts significantly more potent antitumor activity against peritoneal dissemination of scirrhous gastric cancer cells than CPT-11, indicating the possibility of the clinical evaluation of this drug in patients with disseminated gastric cancer.

Disclosure of Potential Conflicts of Interest

No potential conflicts of interest were disclosed.

Acknowledgments

Received 7/23/2008; revised 9/2/2008; accepted 9/16/2008.

Grant support: Third Term Comprehensive Control Research for Cancer from the Ministry of Health, Labor and Welfare of Japan (Y. Matsumura) and a Grant-in-Aid for Scientific Research on Priority Areas from the Ministry of Education, Culture, Sports, Science and Technology (Y. Matsumura).

The costs of publication of this article were defrayed in part by the payment of page charges. This article must therefore be hereby marked *advertisement* in accordance with 18 U.S.C. Section 1734 solely to indicate this fact.

References

- Koizumi W, Narahara H, Hara T, et al. S-1 plus cisplatin versus S-1 alone for first-line treatment of advanced gastric cancer (SPIRITS trial): a phase III trial. *Lancet Oncol* 2008;9:215–21.
- Maehara Y, Moriguchi S, Orita H, et al. Lower survival rate for patients with carcinoma of the stomach of Borrmann type IV after gastric resection. *Surg Gynecol Obstet* 1992;175:13–6.
- Yonemura Y. Mechanisms of drug resistance in gastric cancer. In: Yonemura Y, editor. *Contemporary Approaches Toward Cure of Gastric Cancer*. Kanazawa: Maeda Shoten Co. Ltd.; 1996. p. 87–91.
- Yashiro M, Chung YS, Nishimura S, Inoue T, Sowa M. Fibrosis in the peritoneum induced by scirrhous gastric cancer cells may act as "soil" for peritoneal dissemination. *Cancer* 1996;77:1668–75.
- Jain RK. Barriers to drug delivery in solid tumors. *Sci Am* 1994;271:58–65.
- Senger DR, Galli SJ, Dvorak AM, Perruzzi CA, Harvey VS, Dvorak HF. Tumor cells secrete a vascular permeability factor that promotes accumulation of ascites fluid. *Science* 1983;219:983–5.
- Dvorak HF, Brown LF, Detmar M, Dvorak AM. Vascular permeability factor/vascular endothelial growth factor, microvascular hyperpermeability, and angiogenesis. *Am J Pathol* 1995;146:1029–39.
- Nagy JA, Masse EM, Herzberg KT, et al. Pathogenesis of ascites tumor growth: vascular permeability factor, vascular hyperpermeability, and ascites fluid accumulation. *Cancer Res* 1995;55:360–8.
- Boocock CA, Charnock-Jones DS, Sharkey AM, et al. Expression of vascular endothelial growth factor and its receptors flt and KDR in ovarian carcinoma. *J Natl Cancer Inst* 1995;87:506–16.
- Aoyagi K, Kouhji K, Yano S, et al. VEGF significance in peritoneal recurrence from gastric cancer. *Gastric Cancer* 2005;8:155–63.
- Maeda H, Matsumura Y, Kato H. Purification and identification of [hydroxypropyl]3bradykinin in ascitic fluid from a patient with gastric cancer. *J Biol Chem* 1988;263:16051–4.
- Matsumura Y, Maruo K, Kimura M, Yamamoto T, Konno T, Maeda H. Kinin-generating cascade in advanced cancer patients and *in vitro* study. *Jpn J Cancer Res* 1991;82:732–41.
- Wu J, Akaike T, Hayashida K, et al. Identification of bradykinin receptors in clinical cancer specimens and murine tumor tissues. *Int J Cancer* 2002;98:29–35.
- Matsumura Y, Maeda H. A new concept for macromolecular therapeutics in cancer chemotherapy: mechanism of tumorotropic accumulation of proteins and the antitumor agent smancs. *Cancer Res* 1986;46:6387–92.
- Koizumi F, Kitagawa M, Negishi T, et al. Novel SN-38-incorporating polymeric micelles, NK012, eradicate vascular endothelial growth factor-secreting bulky tumors. *Cancer Res* 2006;66:10048–56.
- Nakajima TE, Yasunaga M, Kano Y, et al. Synergistic antitumor activity of the novel SN-38-incorporating polymeric micelles, NK012, combined with 5-fluorouracil in a mouse model of colorectal cancer, as compared with that of irinotecan plus 5-fluorouracil. *Int J Cancer* 2008;122:2148–53.
- Saito Y, Yasunaga M, Kuroda J, Koga Y, Matsumura Y. Enhanced distribution of NK012, a polymeric micelle-encapsulated SN-38, and sustained release of SN-38 within tumors can beat a hypovascular tumor. *Cancer Sci* 2008;99:1258–64.
- Yanagihara K, Takigahira M, Tanaka H, et al. Development and biological analysis of peritoneal metastasis mouse models for human scirrhous stomach cancer. *Cancer Sci* 2005;96:323–32.
- Yanagihara K, Takigahira M, Takeshita F, et al. A photon counting technique for quantitatively evaluating progression of peritoneal tumor dissemination. *Cancer Res* 2006;66:7532–9.
- Yanagihara K, Tanaka H, Takigahira M, et al. Establishment of two cell lines from human gastric scirrhous carcinoma that possess the potential to metastasize spontaneously in nude mice. *Cancer Sci* 2004;95:575–82.
- Arao T, Yanagihara K, Takigahira M, et al. ZD6474 inhibits tumor growth and intraperitoneal dissemination in a highly metastatic orthotopic gastric cancer model. *Int J Cancer* 2006;118:483–9.
- Slatter JG, Schaaf LJ, Sams JR, et al. Pharmacokinetics, metabolism, and excretion of irinotecan (CPT-11) following I.V. infusion of [(14)C]CPT-11 in cancer patients. *Drug Metab Dispos* 2000;28:423–33.
- Rothenberg ML, Kuhn JG, Burris HA III, et al. Phase I and pharmacokinetic trial of weekly CPT-11. *J Clin Oncol* 1993;11:2194–204.
- Guichard S, Terret C, Hennebelle I, et al. CPT-11 converting carboxylesterase and topoisomerase activities in tumour and normal colon and liver tissues. *Br J Cancer* 1999;80:364–70.
- Kawato Y, Aonuma M, Hirota Y, Kuga H, Sato K. Intracellular roles of SN-38, a metabolite of the camptothecin derivative CPT-11, in the antitumor effect of CPT-11. *Cancer Res* 1991;51:4187–91.
- Araki E, Ishikawa M, Iigo M, Koide T, Itabashi M, Hoshi A. Relationship between development of diarrhea and the concentration of SN-38, an active metabolite of CPT-11, in the intestine and the blood plasma of athymic mice following intraperitoneal administration of CPT-11. *Jpn J Cancer Res* 1993;84:697–702.
- Atsumi R, Suzuki W, Hokusui H. Identification of the metabolites of irinotecan, a new derivative of camptothecin, in rat bile and its biliary excretion. *Xenobiotica* 1991;21:1159–69.
- Kato K, Hamaguchi T, Shirao K, et al. Interim analysis of phase I study of NK012, polymer micelle SN-38, in patients with advanced cancer. *Proc Am Soc Clin Oncol GI* 2008 (Abs #485).
- Burris HA III, Infante JR, Spigel DR, et al. A phase I dose-escalation study of NK012. *Proc Am Soc Clin Oncol* 2008 (Abs #2358).

Synergistic antitumor activity of the novel SN-38-incorporating polymeric micelles, NK012, combined with 5-fluorouracil in a mouse model of colorectal cancer, as compared with that of irinotecan plus 5-fluorouracil

Takako Eguchi Nakajima^{1,2}, Masahiro Yasunaga², Yasuhiko Kano³, Fumiaki Koizumi⁴, Ken Kato¹, Tetsuya Hamaguchi¹, Yasuhide Yamada¹, Kuniaki Shirao¹, Yasuhiro Shimada¹ and Yasuhiro Matsumura^{2*}

¹Gastrointestinal Oncology Division, National Cancer Center Hospital, Tokyo, Japan

²Investigative Treatment Division, Research Center for Innovative Oncology, National Cancer Center Hospital East, Kashiwa, Chiba, Japan

³Hematology Oncology, Tochigi Cancer Center, Tochigi, Japan

⁴Shien Lab Medical Oncology Division, National Cancer Center Hospital, Tokyo, Japan

The authors reported in a previous study that NK012, a 7-ethyl-10-hydroxy-camptothecin (SN-38)-releasing nano-system, exhibited high antitumor activity against human colorectal cancer xenografts. This study was conducted to investigate the advantages of NK012 over irinotecan hydrochloride (CPT-11) administered in combination with 5-fluorouracil (5FU). The cytotoxic effects of NK012 or SN-38 (an active metabolite of CPT-11) administered in combination with 5FU was evaluated *in vitro* in the human colorectal cancer cell line HT-29 by the combination index method. The effects of the same drug combinations was also evaluated *in vivo* using mice bearing HT-29 and HCT-116 cells. All the drugs were administered i.v. 3 times a week; NK012 (10 mg/kg) or CPT11 (50 mg/kg) was given 24 hr before 5FU (50 mg/kg). Cell cycle analysis in the HT-29 tumors administered NK012 or CPT-11 *in vivo* was performed by flow cytometry. NK012 exerted more synergistic activity with 5FU compared to SN-38. The therapeutic effect of NK012/5FU was significantly superior to that of CPT-11/5FU against HT-29 tumors ($p = 0.0004$), whereas no significant difference in the antitumor effect against HCT-116 tumors was observed between the 2-drug combinations ($p = 0.2230$). Cell-cycle analysis showed that both NK012 and CPT-11 tend to cause accumulation of cells in the S phase, although this effect was more pronounced and maintained for a more prolonged period with NK012 than with CPT-11. Optimal therapeutic synergy was observed between NK012 and 5FU, therefore, this regimen is considered to hold promise of clinical benefit, especially for patients with colorectal cancer.

© 2008 Wiley-Liss, Inc.

Key words: NK012; SN-38; 5-fluorouracil; drug delivery system; colorectal cancer

The 5-year survival rates of colorectal cancer (CRC) have improved remarkably over the last 10 years, accounted for in large part by the extensively investigated agents after 5-fluorouracil (5FU). Irinotecan hydrochloride (CPT-11), a water-soluble, semi-synthetic derivative of camptothecin, is one such agent that has been shown to be highly effective, and currently represents a key-drug in first- and second-line treatment regimens for CRC. CPT-11 monotherapy, however, has not been shown to yield superior efficacy, including in terms of the median survival time, to bolus 5FU/leucovorin (LV) alone.¹ In 2 Phase III trials, the addition of CPT-11 to bolus or infusional 5FU/LV regimens clearly yielded greater efficacy than administration of 5FU/LV alone, with a doubling of the tumor response rate and prolongation of the median survival time by 2–3 months.^{1,2}

CPT-11 is converted to 7-ethyl-10-hydroxy-camptothecin (SN-38), a biologically active and water-insoluble metabolite of CPT-11, by carboxylesterases in the liver and the tumor. SN-38 has been demonstrated to exhibit up to a 1,000-fold more potent cytotoxic activity than CPT-11 against various cancer cells *in vitro*.³ The metabolic conversion rate is, however, very low, with only <10% of the original volume of CPT-11 being metabolized to SN-38^{4,5}; conversion of CPT-11 to SN-38 also depends on genetic interindividual variability of the activity of carboxylesterases.⁶

Direct use of SN-38 itself for clinical cancer treatment must be shown to be identical in terms of both efficacy and toxicity.

Some drugs incorporated in drug delivery systems (DDS), such as Abraxane and Doxil, are already in clinical use.^{7,8} The clinical benefits of DDS are based on their EPR effect.⁹ The EPR effect is based on the pathophysiological characteristics of solid tumor tissues: hypervascularity, incomplete vascular architecture, secretion of vascular permeability factors stimulating extravasation within cancer tissue, and absence of effective lymphatic drainage from the tumors that impedes the efficient clearance of macromolecules accumulated in solid tumor tissues. Several types of DDS can be used for incorporation of a drug. A liposome-based formulation of SN-38 (LE-SN38) has been developed, and a clinical trial to assess its efficacy is now under way.^{10,11}

Recently, we demonstrated that NK012, novel SN-38-incorporating polymeric micelles, exerted superior antitumor activity and less toxicity than CPT-11.¹² NK012 is characterized by a smaller size of the particles than LE-SN38; the mean particle diameter of NK012 is 20 nm. NK012 can release SN-38 under neutral conditions even in the absence of a hydrolytic enzyme, because the bond between SN-38 and the block copolymer is a phenol ester bond, which is stable under acidic conditions and labile under mild alkaline conditions. The release rate of SN-38 from NK012 under physiological conditions is quite high; more than 70% of SN-38 is released within 48 hr. We speculated that the use of NK012, in place of CPT-11, in combination with 5FU may yield superior results in the treatment of CRC. In the present study, we evaluated the antitumor activity of NK012 administered in combination with 5FU as compared to that of CPT-11 administered in combination with 5FU against CRC in an experimental model.

Material and methods

Cells and animals

The human colorectal cancer cell lines used, namely, HT-29 and HCT-116, were purchased from the American Type Culture Collection (Rockville, MD). The HT-29 cells and HCT-116 cells were maintained in RPMI 1640 supplemented with 10% fetal bovine serum (Cell Culture Technologies, Gagnenau-Hoerden, Germany), penicillin, streptomycin, and amphotericin B (100 units/mL, 100 µg/mL, and 25 µg/mL, respectively; Sigma, St. Louis, MO) in a humidified atmosphere containing 5% CO₂ at 37°C.

BALB/c *nu/nu* mice were purchased from SLC Japan (Shizuoka, Japan). Six-week-old mice were subcutaneously (s.c.)

*Correspondence to: Investigative Treatment Division, Research Center for Innovative Oncology, National Cancer Center Hospital East, 6-5-1 Kashiwanoha, Kashiwa, Chiba 277-8577, Japan. Fax: +81-4-7134-6866. E-mail: yhmatsum@east.ncc.go.jp

Received 2 September 2007; Accepted after revision 20 November 2007
DOI 10.1002/ijc.23381

Published online 14 January 2008 in Wiley InterScience (www.interscience.wiley.com).

inoculated with 1×10^6 cells of HT-29 or HCT-116 cell line in the flank region. The length (a) and width (b) of the tumor masses were measured twice a week, and the tumor volume (TV) was calculated as follows: $TV = (a \times b^2)/2$. All animal procedures were performed in compliance with the Guidelines for the Care and Use of Experimental Animals established by the Committee for Animal Experimentation of the National Cancer Center; these guidelines meet the ethical standards required by law and also comply with the guidelines for the use of experimental animals in Japan.

Drugs

The SN-38-incorporating polymeric micelles, NK012, and SN-38 were prepared by Nippon Kayaku (Tokyo, Japan).¹² CPT-11 was purchased from Yakult Honsha (Tokyo, Japan). 5FU was purchased from Kyowa Hakko (Tokyo, Japan).

Cell growth inhibition assay

HT-29 cells were seeded in 96-well plates at a density of 2,000 cells/well in a final volume of 90 μ L. Twenty-four hours after seeding, a graded concentration of NK012 or SN-38 was added concurrently with 5FU to the culture medium of the HT-29 cells in a final volume of 100 μ L for drug interaction studies. The culture was maintained in the CO₂ incubator for an additional 72 hr. Then, cell growth inhibition was measured by the tetrazolium salt-based proliferation assay (WST assay; Wako Chemicals, Osaka, Japan). WST-1 labeling solution (10 μ L) was added to each well and the plates were incubated at 37°C for 3 hr. The absorbance of the formazan product formed was detected at 450 nm in a 96-well spectrophotometric plate reader. Cell viability was measured and compared to that of the control cells. Each experiment was carried out in triplicate and was repeated at least 3 times. Data were averaged and normalized against the nontreated controls to generate dose-response curves.

Drug interaction analysis

The nature of interaction between NK012 or SN-38 and 5FU against HT-29 cells was evaluated by median-effect plot analyses and the combination index (CI) method of Chou and Talalay.¹³ Data analysis was performed using the CalcuSyn software (BioSoft, NY, USA). NK012 or SN-38 was combined with 5FU at a fixed ratio that spanned the individual IC₅₀ values of each drug. The IC₅₀ values were determined on the basis of the dose-response curves using the WST assay. For any given drug combination, the CI is known to represent the degree of synergy, additivity or antagonism. It is expressed in terms of fraction-affected (F_a) values, which represents the percentage of cells killed or inhibited by the drug. Isobologram equations and F_a/CI plots were constructed by computer analysis of the data generated from the median effect analysis. Each experiment was performed in triplicate with 6 gradations and was repeated at least 3 times. The resultant dose-response curves were averaged, to create a single composite dose-response curve for each combination.

In vivo analysis of the effects of NK012 combined with 5FU as compared to those of CPT-11 combined with 5FU

When the mean tumor volumes reached ~ 93 mm³, the mice were randomly divided into test groups consisting of 5 mice per group (Day 0). The drugs were administered i.v. via the tail vein of the mice. In the groups administered NK012 or 5FU as single agents, the drug was administered on Days 0, 7 and 14. In the combined treatment groups, NK012 or CPT-11 was administered 24 hr before 5FU on Days 0, 7 and 14, according to the previously reported combination schedule for CPT-11 and 5FU.¹⁴ Complete response (CR) was defined as tumor not detectable by palpation at 90 days after the start of treatment, at which time-point the mice were sacrificed. Tumor volume and body weight were measured twice a week. As a general rule, animals in which the tumor volume exceeded 2,000 mm³ were also sacrificed.

Experiment 1. Evaluation of the effects of NK012 combined with 5FU and determination of the maximum tolerated dose (MTD) of NK012/5FU. By comparing the data between NK012 administered as a single agent and NK012/5FU, we evaluated the effects of the combined regimen against the s.c. HT-29 tumors. A preliminary experiment showed that combined administration of NK012 15 mg/kg + 5FU 50 mg/kg every 6 days caused drug-related lethality (data not shown). To determine the MTD, therefore, we set the dosing schedule of the combined regimen at 5 or 10 mg/kg of NK012 + 50 mg/kg of 5FU three times a week.

Experiment 2. Comparison of the antitumor effect of NK012/5FU and CPT-11/5FU. Based on a comparison of the data between NK012/5FU and CPT-11/5FU against the s.c. HT-29 and HCT-116 tumors, we investigated the feasibility of the clinical application of NK012/5FU for the treatment of CRC. CPT-11/5FU was administered three times a week at the respective MTDs of the 2 drugs as previously reported, that is, CPT-11 at 50 mg/kg and 5FU at 50 mg/kg, respectively.¹⁴ NK012/5FU was administered once three times a week at the respective MTDs of the 2 drugs determined from Experiment 1.

Cell cycle analysis

Samples from the HT-29 tumors that had grown to 80–100 mm³ were removed from the mice at 6, 24, 48, 72 and 96 hr after the administration of NK012 alone at 10 mg/kg or CPT-11 alone at 50 mg/kg. The samples were excised, minced in PBS and fixed in 70% ethanol at -20°C for 48 hr. They were then digested with 0.04% pepsin (Sigma chemical Co., St Louis, MO) in 0.1 N HCL for 60 min at 37°C in a shaking bath to prepare single-nuclei suspensions. The nuclei were then centrifuged, washed twice with PBS and stained with 40 μ g/mL of propidium iodide (Molecular Probes, OR) in the presence of 100 μ g/mL RNase in 1 mL PBS for 30 min at 37°C. The stained nuclei were analyzed with B-D FACSCalibur (BD Biosciences, San Jose, CA), and the cell cycle distribution was analyzed using the Modfit program (Verity Software House Topsham, ME).

Statistical analyses

Data were expressed as mean \pm SD. Data were analysed with Student's t test when the groups showed equal variances (F test), or Welch's test when they showed unequal variances (F test). $p < 0.05$ was regarded as statistically significant. All statistical tests were 2-sided.

Results

Antiproliferative effects of NK012 or SN-38 administered in combination with 5FU

Figure 1a shows the dose-response curves for NK012 alone, 5FU alone and a combination of the two. The IC₅₀ levels of NK012 and 5FU against the HT-29 cells were 39 nM and 1 μ M, respectively, and the IC₅₀ level of SN-38 was 14 nM (data not shown). Based on these data, the molar ratio of NK012 or SN-38:5FU of 1:1,000 was used for the drug combination studies.

Figures 1b and 1c show the median-effect and the combination index plots. Combination indices (CIs) of <1.0 are indicative of synergistic interactions between 2 agents; additive interactions are indicated by CIs of 1.0, and antagonism by CIs of >1.0 . Figure 1c shows the combination index for NK012 and 5FU, when 2 drugs are supposed to be mutually exclusive. Marked synergism was observed between F_a 0.2 and 0.6. Theoretically, the CI method is the most reliable around an F_a of 0.5, suggesting synergistic effects of the combination of NK012 and 5FU. This synergistic effect was more evident than that of SN-38/5FU (Fig. 1d).

In vivo effect of combined NK012 and 5FU

Experiment 1. Dose optimization and effect of combined NK012 and 5FU against HT-29 tumors. Comparison of the relative tumor volumes on Day 40 revealed significant differences between

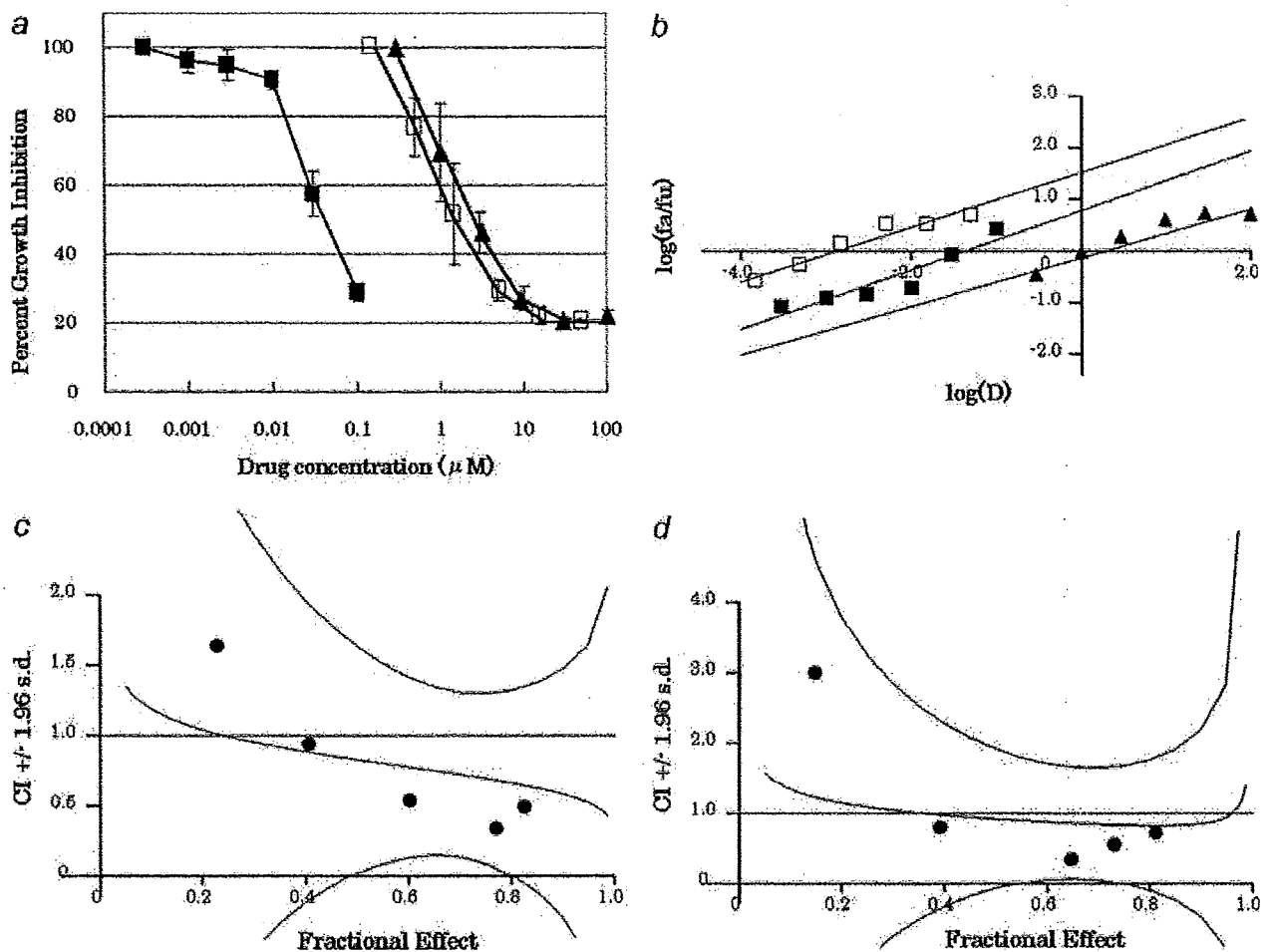


FIGURE 1 – Interaction of NK012 and 5FU *in vitro*. (a) Dose-response curves for NK012 alone (■), 5FU alone (▲) and their combination (□) against HT-29 cells. HT-29 cells were seeded at 2,000 cells/well. Twenty-four hours after seeding, a graded concentration of NK012 or 5FU was added to the culture medium of the HT-29 cells. Cell growth inhibition was measured by WST assay after 72 hr of treatment. Cell viability was measured and compared with that of the control cells. Each experiment was carried out independently and repeated at least 3 times. Points, mean of triplicates; bars, SD. (b) Median effect plot for the interaction of NK012 and 5FU. (c, d) Combination index for the interaction as a function of the level of effect (fraction effect = 0.5 is the IC_{50}). The straight line across the CI value of 1.0 indicates additive effect and CIs above and below indicate antagonism and synergism, respectively. The molar ratio of NK012/5FU (c) or SN-38/5FU (d) at 1:1,000 was tested by CI analysis. Black circles represent the CIs of the actual data points, solid lines represent the computer-derived CIs at effect levels ranging from 10 to 100% inhibition of cell growth, and the dotted lines represent the 95% confidence intervals.

those in the mice administered NK012 alone and those administered NK012/5FU at 5 mg/kg of NK012 ($p = 0.018$) (Fig. 2a). Although there was no statistically significant difference in the relative tumor volume measured on Day 54 between the mice administered NK012 alone and NK012/5FU at 10 mg/kg of NK012 ($p = 0.3050$), a trend of superior antitumor effect was demonstrated in the group treated with NK012/5FU at 10 mg/kg of NK012 (Fig. 2a). The CR rates were 20, 40 and 60% for 5 mg/kg NK012 + 50 mg/kg 5FU, 10 mg/kg NK012 alone and 10 mg/kg NK012 + 50 mg/kg 5FU, respectively. The schedule of 10 mg/kg NK012 + 50 mg/kg 5FU resulted in no remarkable toxicity in terms of body weight changes, and these doses were determined as representing the MTDs (Fig. 2b).

Experiment 2. Comparison of the antitumor effect of combined NK012/5FU and CPT-11/5FU against HT-29 and HCT-116 tumors. The therapeutic effect of NK012/5FU on Day 60 was significantly superior to that of CPT-11/5FU against the HT-29 tumors ($p = 0.0004$) (Fig. 3a). A more potent antitumor effect, namely, a 100% CR rate, was obtained in the NK012/5FU group as compared to the 0% CR rate in the CPT-11/5FU group. Although no statistically significant difference in the relative tumor volume on Day 61 was demonstrated between the NK012/

5FU and CPT-11/5FU in the case of the HCT-116 tumors ($p = 0.2230$), a trend of superior antitumor effect against these tumors was observed in the NK012/5FU treatment group (Fig. 3b). The CR rates for the case of the HCT-116 tumors were 0% in both NK012/5FU and CPT-11/5FU groups.

Specificity of cell cycle perturbation

We studied the differences in the effects between NK012 10 mg/kg and CPT-11 50 mg/kg on the cell cycle (Fig. 4a). The data indicated that both NK012 and CPT-11 tended to cause accumulation of cells in the S phase, although the effect of NK012 was stronger and maintained for a more prolonged period than that of CPT-11; the maximal percentage of S-phase cells in the total cell population in the tumors was 34% at 24 hr after the administration of CPT-11, whereas it was 39% at 48 hr after the administration of NK012 (Figs. 4b, and 4c).

Discussion

Our primary endpoint was to clarify the advantages of NK012 over CPT-11 administered in combination with 5FU. We demonstrated that combined NK012 and 5FU chemotherapy exerts more

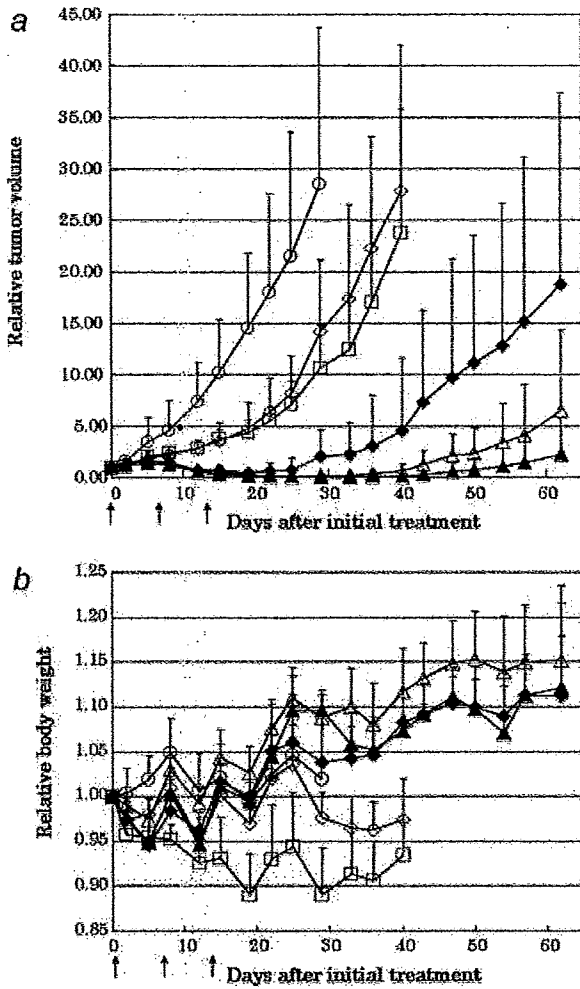


FIGURE 2 – Effect of NK012 alone or NK012 in combination with 5FU against HT-29 tumor-bearing mice. Points, mean; bars, SD. (a) Antitumor effect of each regimen on Days 0, 7 and 14. (○) control, (□) 5FU 50 mg/kg alone, (◇) NK012 5 mg/kg alone, (◆) NK012 5 mg/kg 24 hr before 5FU 50 mg/kg, (△) NK012 10 mg/kg alone, (▲) NK012 10 mg/kg 24 hr before 5FU 50 mg/kg. (b) Changes in the relative body weight. Data were derived from the same mice as those used in the present study.

synergistic activity *in vitro* and significantly greater antitumor activity against human CRC xenografts as compared to CPT-11/5FU. The combination of NK012 and 5FU is considered to hold promise of clinical benefit for patients with CRC.

CPT-11, a topoisomerase-I inhibitor, and 5FU, a thymidilate synthase inhibitor, have been demonstrated to be effective agents for the treatment of CRC. A combination of these 2 drugs has also been demonstrated to be clearly more effective than either CPT-11 or 5FU/LV administered alone *in vivo* and in clinical settings.^{1,2,14} Administration of 5FU by infusion with CPT-11 was shown to be associated with reduced toxicity and an apparent improvement in survival as compared to that of administration of the drug by bolus injection with CPT-11.^{1,2} This synergistic enhancement may result from the mechanism of action of the 2 drugs; CPT-11 has been reported to cause accumulation of cells in the S phase, and 5FU infusion is known to cause DNA damage specifically in cells of the S phase.¹⁴ On the basis of this background, our results suggesting the more pronounced and more prolonged accumulation of the tumor cells in the S phase caused by NK012 as compared with that by CPT-11 may explain the more effective synergy of the former administered with 5FU infusion.

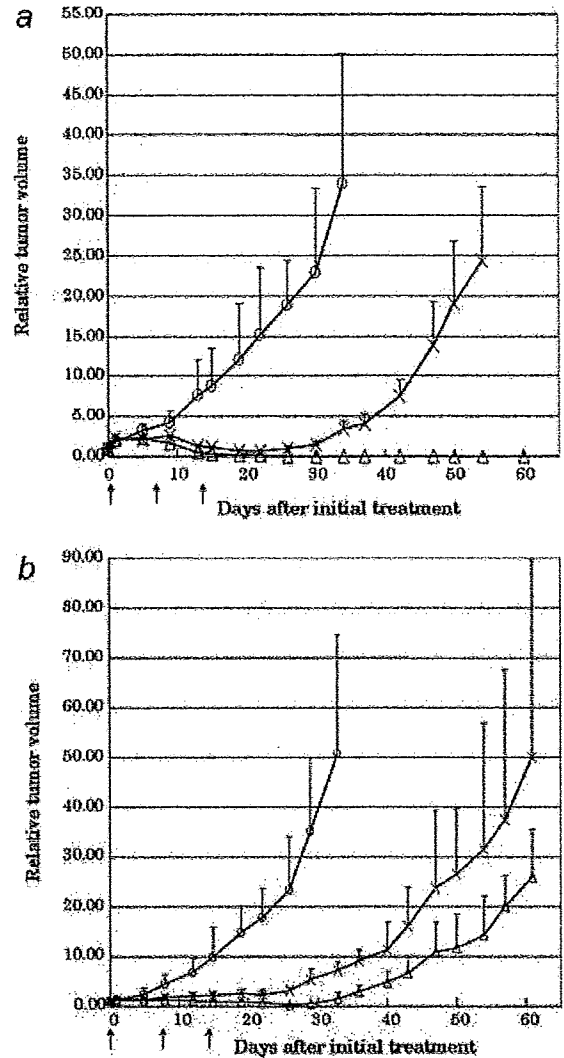
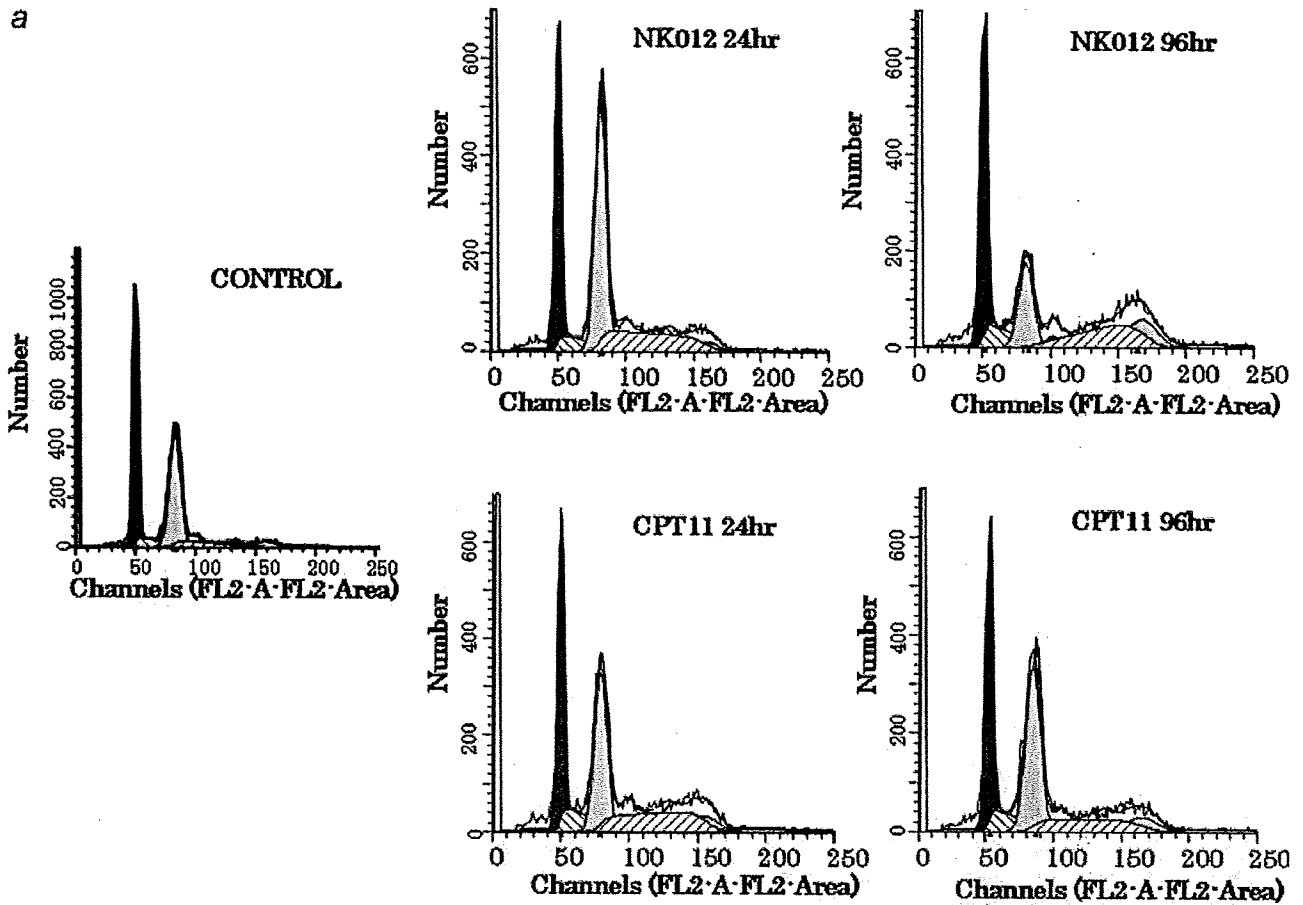


FIGURE 3 – Effect of NK012/5FU as compared with that of CPT11/5FU against HT-29 (a) or HCT-116 (b) tumor-bearing mice. Antitumor effect of each schedule on Days 0, 7 and 14. (○) control, (×) CPT-11 50 mg/kg 24 hr before 5FU 50 mg/kg, (△) NK012 10 mg/kg 24 hr before 5FU 50 mg/kg. Points, mean; bars, SD.

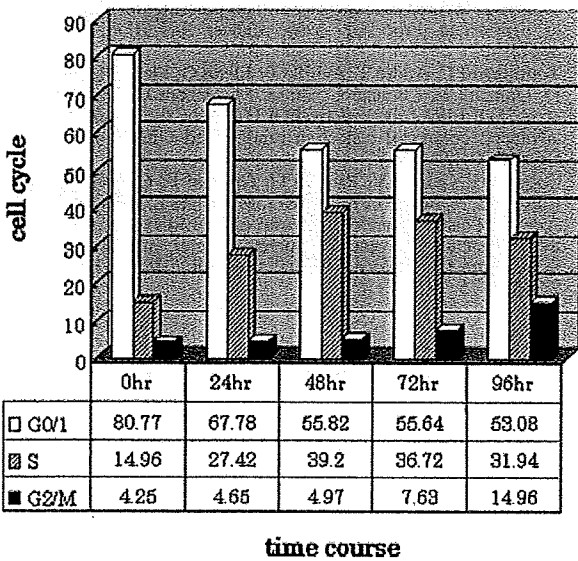
This may be attributable to accumulation of NK012 due to the enhanced permeability and retention (EPR) effect.⁹ It is also speculated that NK012 allows sustained release of free SN-38, which may move more freely in the tumor interstitium.¹⁵ Otherwise NK012 itself could internalize into cells to localize in several cytoplasmic organelles as reported by Savic *et al.*¹⁶ These characteristics of NK012 may be responsible for its more potent antitumor activity observed in this study, because CPT-11 has been reported to show time-dependent growth-inhibitory activity against the tumor cells.¹⁷

The major dose-limiting toxicities of CPT-11 are diarrhea and neutropenia. SN-38, the active metabolite of CPT-11, may cause CPT-11-related diarrhea as a result of mitotic -inhibitory activity.¹⁸ Because it undergoes significant biliary excretion, SN-38 may have a potentially long residence time in the gastrointestinal tract that may be associated with prolonged diarrhea.^{19,20} In our previous report, we evaluated the tissue distribution of SN-38 after administration of an equimolar amount of NK012 (20 mg/kg) and CPT-11 (30 mg/kg), and found no difference in the level of SN-38 accumulation in the small intestine.¹² A significant antitumor effect of NK012 with a lower incidence of diarrhea was also dem-

a



b



c

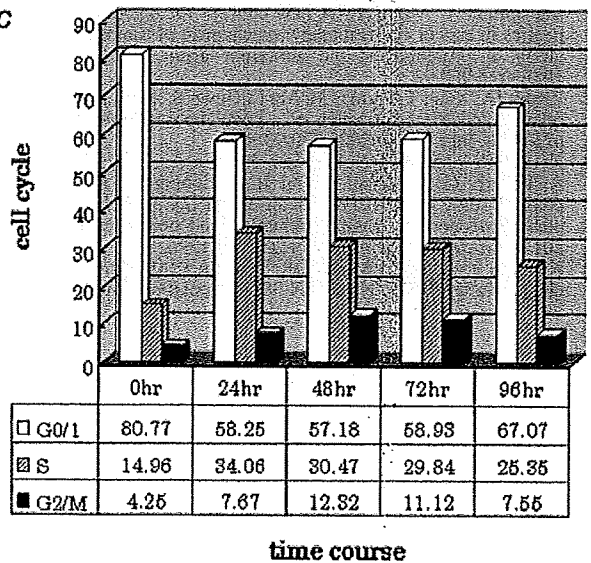


FIGURE 4 – Cell cycle analysis of HT-29 tumor cells collected 24, 48, 72 and 96 hr after administration of NK012 at 10 mg/kg alone or CPT-11 at 50 mg/kg alone using the Modfit program (Verity Software House Topsham, ME). (a) Cell cycle analysis of HT-29 tumor cells 24 and 96 hr after administration of NK012 at 10 mg/kg or CPT-11 at 50 mg/kg, respectively. (b) Cell cycle distribution of tumor cells 0, 24, 48, 72 and 96 hr after treatment with NK012 at 10 mg/kg. (c) Cell cycle distribution of tumor cells 0, 24, 48, 72 and 96 hr after treatment with CPT-11 at 50 mg/kg.

onstrated as compared to that observed with CPT-11 in a rat mammary tumor model.²¹ Combined administration of CPT-11 with 5FU/LV infusion appears to be associated with acceptable toxicity in patients with CRC. In addition, no significant difference in the frequency of Grade 3/4 diarrhea was noted between patients

treated with FOLFIRI (CPT-11 regimen with bolus and infusional 5FU/LV) and those treated with FOLFOX6 (oxaliplatin regimen with bolus and infusional 5FU/LV).^{22,23} Our *in vivo* data actually revealed no severe body weight loss in the NK012/5FU group. Consequently, we expect that the NK012/5FU regimen, especially

with infusional 5FU, may be an attractive arm for a Phase III trial in CRC, with CPT-11/5FU as the control arm. We have already initiated a Phase I trial of NK012 in patients with advanced solid tumors based on the data suggesting higher efficacy and lower toxicity of this preparation than CPT-11 *in vivo*.¹²

In conclusion, we demonstrated that combined NK012 and 5FU chemotherapy exerts significantly greater antitumor activity against human CRC xenografts as compared to CPT-11/5FU, indicating the necessity of clinical evaluation of this combined regimen.

References

- Saltz LB, Douillard JY, Pirotta N, Alakl M, Gruia G, Awad L, Elfring GL, Locker PK, Miller LL. Irinotecan plus fluorouracil/leucovorin for metastatic colorectal cancer: a new survival standard. *Oncologist* 2001;6:81-91.
- Douillard JY, Cunningham D, Roth AD, Navarro M, James RD, Karasek P, Jandik P, Iveson T, Carmichael J, Alakl M, Gruia G, Awad L, et al. Irinotecan combined with fluorouracil compared with fluorouracil alone as first-line treatment for metastatic colorectal cancer: a multicentre randomised trial. *Lancet* 2000;355:1041-7.
- Takimoto CH, Arbuck SG. Topoisomerase I targeting agents: the camptothecins. In: Chabner BA, Lango DL, eds. *Cancer chemotherapy and biotherapy: principal and practice*, 3rd ed. Philadelphia, PA: Lippincott Williams and Wilkins, 2001. 579-646.
- Slatter JG, Schaaf LJ, Sams JP, Feenstra KL, Johnson MG, Bombardt PA, Cathcart KS, Verburg MT, Pearson LK, Compton LD, Miller LL, Baker DS, et al. Pharmacokinetics, metabolism, and excretion of irinotecan (CPT-11) following I.V. infusion of [(14)C]CPT-11 in cancer patients. *Drug Metab Dispos* 2000;28:423-33.
- Rothenberg ML, Kuhn JG, Burris HA, III, Nelson J, Eckardt JR, Tristan-Morales M, Hilsenbeck SG, Weiss GR, Smith LS, Rodriguez GI, Rock MK, Von Hoff DD. Phase I and pharmacokinetic trial of weekly CPT-11. *J Clin Oncol* 1993;11:2194-204.
- Guichard S, Terret C, Hennebelle I, Lochon I, Chevreau P, Fretigny E, Selves J, Chatelut E, Bugat R, Canal P. CPT-11 converting carboxylesterase and topoisomerase activities in tumour and normal colon and liver tissues. *Br J Cancer* 1999;80:364-70.
- Gradishar WJ, Tjulandin S, Davidson N, Shaw H, Desai N, Bhar P, Hawkins M, O'Shaughnessy J. Phase III trial of nanoparticle albumin-bound paclitaxel compared with polyethylated castor oil-based paclitaxel in women with breast cancer. *J Clin Oncol* 2005;23:7794-803.
- Muggia FM. Liposomal encapsulated anthracyclines: new therapeutic horizons. *Curr Oncol Rep* 2001;3:156-62.
- Matsumura Y, Maeda H. A new concept for macromolecular therapeutics in cancer chemotherapy: mechanism of tumoritropic accumulation of proteins and the antitumor agent smancs. *Cancer Res* 1986;46:6387-92.
- Zhang JA, Xuan T, Parmar M, Ma L, Ugwu S, Ali S, Ahmad I. Development and characterization of a novel liposome-based formulation of SN-38. *Int J Pharm* 2004;270:93-107.
- Kraut EH, Fishman MN, LoRusso PM, Gorden MS, Rubin EH, Haas A, Fetterly GJ, Cullinan P, Dul JL, Steinberg JL. Final result of a phase I study of liposome encapsulated SN-38 (LE-SN38): safety, pharmacogenomics, pharmacokinetics, and tumor response [abstract 2017]. *Proc Am Soc Clin Oncol* 2005;23:139S.
- Koizumi F, Kitagawa M, Negishi T, Onda T, Matsumoto S, Hamaguchi T, Matsumura Y. Novel SN-38-incorporating polymeric micelles. NK012, eradicate vascular endothelial growth factor-secreting bulky tumors. *Cancer Res* 2006;66:10048-56.
- Chou TC, Talalay P. Quantitative analysis of dose-effect relationships: the combined effects of multiple drugs or enzyme inhibitors. *Adv Enzyme Regul* 1984;22:27-55.
- Azrak RG, Cao S, Slocum HK, Toth K, Durrani FA, Yin MB, Pendyala L, Zhang W, McLeod HL, Rustum YM. Therapeutic synergy between irinotecan and 5-fluorouracil against human tumor xenografts. *Clin Cancer Res* 2004;10:1121-9.
- Jain RK. Barriers to drug delivery in solid tumors. *Sci Am* 1994;271:58-65.
- Savic R, Luo L, Eisenberg A, Maysinger D. Micellar nanocontainers distribute to defined cytoplasmic organelles. *Science* 2003;300:615-18.
- Kawato Y, Aonuma M, Hirota Y, Kuga H, Sato K. Intracellular roles of SN-38, a metabolite of the camptothecin derivative CPT-11, in the antitumor effect of CPT-11. *Cancer Res* 1991;51:4187-91.
- Slater R, Radstone D, Matthews L, McDaid J, Majeed A. Hepatic resection for colorectal liver metastasis after downstaging with irinotecan improves survival. *Proc Am Soc Clin Oncol* 2003;22(abstract 1287).
- Araki E, Ishikawa M, Iigo M, Koide T, Itabashi M, Hoshi A. Relationship between development of diarrhea and the concentration of SN-38, an active metabolite of CPT-11, in the intestine and the blood plasma of athymic mice following intraperitoneal administration of CPT-11. *Jpn J Cancer Res* 1993;84:697-702.
- Atsumi R, Suzuki W, Hakusui H. Identification of the metabolites of irinotecan, a new derivative of camptothecin, in rat bile and its biliary excretion. *Xenobiotica* 1991;21:1159-69.
- Onda T, Nakamura I, Seno C, Matsumoto S, Kitagawa M, Okamoto K, Nishikawa K, Suzuki M. Superior antitumor activity of NK012, 7-ethyl-10-hydroxycamptothecin-incorporating micellar nanoparticle, to irinotecan. *Proc Am Assoc Cancer Res* 2006;47:720s(abstract 3062).
- Tournigand C, Andre T, Achille E, Lledo G, Flesh M, Mery-Mignard D, Quinaux E, Couteau C, Buysse M, Ganem G, Landi B, Colin P, et al. FOLFIRI followed by FOLFOX6 or the reverse sequence in advanced colorectal cancer: a randomized GERCOR study. *J Clin Oncol* 2004;22:229-37.
- Colucci G, Gebbia V, Paoletti G, Giuliani F, Caruso M, Gebbia N, Carteni G, Agostara B, Pezzella G, Manzione L, Borsellino N, Misino A, et al. Phase III randomized trial of FOLFIRI versus FOLFOX4 in the treatment of advanced colorectal cancer: a multicenter study of the Gruppo Oncologico Dell'Italia Meridionale. *J Clin Oncol* 2005;23:4866-75.

Enhanced distribution of NK012, a polymeric micelle-encapsulated SN-38, and sustained release of SN-38 within tumors can beat a hypovascular tumor

Yohei Saito,^{1,2} Masahiro Yasunaga,¹ Junichiro Kuroda,¹ Yoshikatsu Koga¹ and Yasuhiro Matsumura^{1,3}

¹Investigative Treatment Division, Center for Innovative Oncology, National Cancer Center Hospital East, 6-5-1 Kashiwanoha, Kashiwa, Chiba 277-8577;

²Laboratory of Cancer Biology, Department of Integrated Biosciences, Graduate School of Frontier Sciences, The University of Tokyo, 5-1-5 Kashiwanoha, Kashiwa, Chiba 277-8562, Japan

(Received January 16, 2008/Revised February 14, 2008/Accepted February 14, 2008/Online publication April 21, 2008)

Human pancreatic cancer is generally hypovascular in nature and rich in interstitium. These pathological barriers may contribute to the intractable nature of pancreatic cancer by binding the penetration of anticancer agents throughout the tumor tissue. The aim of the present study was to determine whether NK012 is an appropriate formulation for the treatment of hypovascular tumors. Among pancreatic tumor xenografts, PSN1 appeared to have the richest tumor vasculature and the least number of stromal cells and matrix. In contrast, Capan1 had the poorest tumor vasculature and most abundant stromal tissue. Fluorescence microscopy and high-performance liquid chromatography analysis demonstrated that although NK012 accumulated and continued to be distributed for more than 48 h throughout the entire body of both tumors, CPT-11 disappeared almost entirely from both tumors within 6 h. In addition, efficient sustained release of SN-38 was maintained for more than 96 h in both tumors following administration of NK012. Following the administration of CPT-11, SN-38 was no longer detectable after 24 h in the Capan1 tumor or after 48 h in the PSN1 tumor. All tumors were eradicated in the mice treated with NK012 but not in those treated with CPT-11. Because the antitumor activity of SN-38 is time dependent, NK012, which combines enhanced distribution with sustained release of SN-38 within tumors, may be ideal for the treatment of hypovascular tumors, such as pancreatic cancer. (*Cancer Sci* 2008; 99: 1258–1264)

Pancreatic cancer has one of the worst prognoses among cancers.⁽¹⁾ The median survival of cases of advanced pancreatic cancer is only approximately one in two 1 year after systemic gemcitabine-based chemotherapy.⁽²⁾ The recent success of molecular-targeting agents has also had some impact on pancreatic cancer treatment. A recent phase III trial of gemcitabine alone versus gemcitabine plus erlotinib (a tyrosine kinase inhibitor) in patients with advanced pancreatic cancer showed that overall survival was significantly prolonged in the gemcitabine + erlotinib arm. However, median survival in the gemcitabine + erlotinib arm (6.24 months) was only 10 days longer than in the gemcitabine-alone arm (5.91 months).⁽³⁾ There is therefore an urgent need to develop modalities by which cytotoxic drugs can exert their significant antitumor activity to their full potential and reasonably prolong the overall survival of patients with advanced pancreatic cancer. There may be several reasons why pancreatic cancer is intractable. It is conceivable that anticancer agents are not delivered efficiently enough to the pancreatic cancer cells to kill them. Pancreatic cancer tissue is generally hypovascular in nature,^(4,5) and is rich in stromal cells and extracellular matrix, and these pathological barriers may hinder efficient penetration of the anticancer agents throughout the entire body of the pancreatic cancer.

The role of drug delivery systems (DDS) is to selectively deliver cytotoxic drugs to tumor tissues while lessening their distribution to normal tissues in order to reduce their side effects.^(6–8) However, it is conceivable that satisfactory drug delivery cannot be achieved in cancers having very few tumor vessels and an abundant collagen-rich interstitium. Therefore, a more sophisticated DDS may be needed for efficient delivery of drugs to such types of cancer as pancreatic cancer.

SN-38, a biologically active metabolite of irinotecan hydrochloride (CPT-11), has potent antitumor activity but has not been used clinically because of its water insolubility. NK012, a successful drug formulation composed of SN-38-incorporating polymeric micelles, has been developed recently, and the remarkable antitumor effects of NK012 against the human small cell lung cancer SBC-3, especially the vascular endothelial growth factor (VEGF)-secreting SBC-3-VEGF tumor, has been demonstrated.⁽⁶⁾

In the present study, we clarified the relationship between the tumor vasculature and interstitium using several human pancreatic xenografts, and evaluated the therapeutic effect of NK012 in a hypovascular and hypervascular pancreatic tumor.

Materials and Methods

Drugs and cells. SN-38 and NK012 were synthesized by Nippon Kayaku (Tokyo, Japan). CPT-11 was purchased from Yakult (Tokyo, Japan). The human pancreatic cancer cell lines Panc1, PSN1, BxPC3, and Capan1 were purchased from American Type Culture Collection (Rockville, MD, USA).

Panc1, PSN1, and Capan1 were maintained in Dulbecco's modified Eagle's medium (DMEM) supplemented with 10% fetal bovine serum, streptomycin, and L-glutamine (Sigma, St Louis, MO, USA) in atmosphere of 5% CO₂ at 37°C. BxPC3 were maintained in RPMI-1640 supplemented with 10% fetal bovine serum, streptomycin, and L-glutamine (Sigma) in an atmosphere of 5% CO₂ at 37°C.

Experimental mouse model. Female BALB/c nude mice, 6 weeks old, were purchased from CLEA Japan (Tokyo, Japan). Mice were inoculated subcutaneously in the flank with 1 × 10⁷ cells/300 μL phosphate-buffered saline (PBS). All animal procedures were carried out in compliance with the guidelines for the care and use of experimental animals, laid down by the Committee for Animal Experimentation of the National Cancer Center; these guidelines meet the ethical standards required by law and also comply with the guidelines for the use of experimental animals in Japan.

³To whom correspondence should be addressed. E-mail: yhmatsum@east.ncc.go.jp

Immunohistochemical study of various human pancreatic tumor xenografts. When the tumor volume reached 300 mm³, tumors were excised from the mice and used for immunohistochemical analysis. To stain the blood vessels, the tissues were embedded in Optimal Cutting Temperature Compound (Sakura Finetechnochemical, Tokyo, Japan) and frozen at -80°C until use. Six micrometer-thick tumor sections were prepared using a cryostatic microtome, Tissue-Tek Cryo3 (Sakura Finetechnochemical), and then air dried for 1 h. The sections were soaked in 10% formalin for 15 min, and washed three times with 0.2 M PBS. The sections were then rinsed with ultrapure water. Endogenous peroxidase was blocked with a 0.3% hydrogen peroxide solution in 100% methanol for 20 min. The sections were then rinsed three times with PBS for 3 min each. Non-specific protein binding was blocked with 5% skim milk (BD, Franklin Lakes, NJ, USA) in PBS for 30 min at room temperature. After draining off the skim milk solution, a polyclonal antibody against factor VIII (Zymed Laboratories, South San Francisco, CA, USA) was added at a dilution of 1:50, followed by incubation for 1 h and three rinses with PBS for 5 min each. Biotinylated antirabbit IgG was added at a dilution of 1:50, followed by incubation for 1 h. The sections were rinsed three times with PBS, and Vectastain Elite ABC Reagent (Vector Laboratories, Burlingame, CA, USA) was added for 30 min. The sections were rinsed again three times with PBS and incubated with the 3,3'-diaminobenzidine tetrahydrochloride (DAB+) Liquid System (Dako, Glostrup, Denmark) for 30 s. Finally, the sections were rinsed and counterstained with hematoxylin solution. For staining of type I, III, and IV collagen, tissues were fixed with 4% formalin, and the paraffin sections were prepared by the Tokyo Histopathologic Laboratory (Tokyo, Japan). First, the sections were soaked three times for 5 min each in xylene, and then three times for 3 min each in ethanol to remove the paraffin. The sections were then rinsed with ultrapure water and endogenous peroxidase was blocked with a 0.3% hydrogen peroxide solution in 100% methanol for 20 min, followed by three rinses for 5 min with PBS. Then, Proteinase K (Dako) was added. After the sections were rinsed three times for 5 min each with 0.2 M PBS, non-specific protein binding was blocked with a 1% normal goat serum (Dako) solution in PBS for 30 min at room temperature. Then, after three rinses for 5 min each with PBS, polyclonal rabbit anti type I, III, and IV collagen antibodies (Dako) were added at dilutions of 1:500 (type I collagen), 1:10 000 (type III collagen), and 1:2000 (type IV collagen), followed by incubation for 1 h. The slides were rinsed in PBS and incubated for 30 min with Envision/HRP (Dako) directed against the primary antibody. After further rinsing, the sections were incubated with the DAB+ Liquid System (Dako) for 30 s. Then, after a final rinse, the sections were counterstained with hematoxylin solution.

In vitro growth assay. The growth-inhibitory effects of NK012, SN-38, and CPT-11 were examined using the WST8 assay. Cell suspensions (5000 cells/100 µL) were seeded into a 96-well microtiter plate, which was incubated for 24 h at 37°C. Then, after removal of the medium, 100 µL of medium containing various concentrations of each drug was added to the wells, which were then incubated for 48 h at 37°C. After removal of the medium, 10 µL of WST8 solution and 90 µL of medium were added to the wells, followed by incubation for 4 h at 37°C. The growth-inhibitory effect of each drug was assessed spectrophotometrically (SpectraMax 190; Molecular Devices, Sunnyvale, CA, USA).

Distribution studies of CPT-11 and NK012 in the tumors by fluorescence microscopy. Nude mice bearing PSN1, as a hypervascular tumor model, or Capan1, as a hypovascular tumor model, were used for studying the distribution of NK012 and CPT-11, when the tumors reached 300 mm³ in volume. The maximum tolerated dose (MTD) of NK012 (30 mg/kg) or CPT-11 (66.7 mg/kg) was injected intravenously into the mice. At 1, 6, 24, or 48 h after the injection of NK012 or CPT-11, the mice were administered

fluorescein-labeled *Lycopersicon esculentum* lectin (100 µL/mouse) (Vector Laboratories) for the purpose of visualizing the tumor blood vessels. The tumors were then excised and embedded in Optimal Cutting Temperature Compound and frozen at -80°C before 6 µm-thick sections were prepared using Tissue-Tek Cryo3. The frozen sections were examined under a fluorescence microscope, Biorevo (Keyence, Osaka, Japan), at an excitation wavelength of 377 nm and emission wavelength 447 nm in order to evaluate the distribution of CPT-11 and NK012 within the tumor tissues. Because formulations containing SN-38 bound via ester bonds possess a particular fluorescence, both CPT-11 and NK012 were detected under the same fluorescence conditions.

Distribution studies of free SN-38, CPT-11, and NK012 in the tumors by high-performance liquid chromatography. When PSN1 and Capan1 tumors reached 300 mm³ in volume, NK012 (30 mg/kg) or CPT-11 (66.7 mg/kg) was administered intravenously to the mice. At 1, 6, 24, 72, or 96 h after the injection of NK012 and CPT-11, each tumor was excised. The tumor tissues were rinsed with physiological saline, mixed with 0.1 M glycine-HCl buffer (pH 3.0) in methanol at 5% (w/w) and homogenized. To detect free SN-38 and CPT-11, the tumor samples (100 µL) were mixed with 20 µL of 1 mM phosphoric acid in methanol (1:1), 40 µL ultrapure water, and camptothecin was used as the internal standard (10 ng/mL for free SN-38, 15 ng/mL for CPT-11). The samples were vortexed vigorously for 10 s and filtered through Ultrafree-MC Centrifugal Filter Devices (Millipore, Bedford, MA, USA). Reverse-phase high-performance liquid chromatography (HPLC) was conducted at 35°C on a Mightysil RP-18 GP column (150 × 4.6 mm; Kanto Chemical, Tokyo, Japan). The samples were injected into an Alliance Water 2795 HPLC system (Waters, Milford, MA, USA) equipped with a Waters 2475 multi λ fluorescence detector. The detector was set at 365 and 430 nm (excitation and emission wavelengths, respectively) for CPT-11, and at 365 and 540 nm for SN-38.

For polymer-bound SN-38 detection, SN-38 was released from the conjugate as described previously.⁽⁸⁾ In brief, 100 µL tissue samples were diluted with 20 µL methanol (50% [w/w]) and 20 µL NaOH (0.7 M). The samples were incubated for 15 min at room temperature. After incubation, 20 µL HCl (0.7 M) and 60 µL of internal standard solution was added to the samples, and then the hydrolysate was filtered. The filtrate was applied to the HPLC system.

Polymer-bound SN-38 was determined by subtraction of non-polymer-bound SN-38 from the total SN-38 in the hydrolysate.

Antitumor activity of NK012 and CPT-11 against Capan1 or PSN1 xenografts. When the tumor volume reached approximately 300 mm³ in volume, the mice were divided randomly into test groups consisting of five mice per group (day 0). The drugs were administered on days 0, 4, and 8 by intravenous injection into the tail vein. NK012 was given at a dose of 30 mg/kg (MTD) and CPT-11 was given at a MTD of 66.7 mg/kg as indicated in the optimal schedule reported previously.⁽⁹⁾

The length (L) and width (W) of the tumor mass were measured every 3 days. The tumor volume (TV) was calculated as follows: TV = (L × W²) × 0.5233.

Statistical analysis. Student's *t*-test was used for the statistical analyses. *P* < 0.05 was considered to denote statistical significance.

Results

Density of collagen and the number of tumor blood vessels in the various human pancreatic tumor xenografts. We examined the density of collagen in four pancreatic cancer xenografts (Fig. 1a). Type I collagen was present in the greatest abundance in Capan1 and was least abundance in PSN1. The density of type I collagen in Panc1 and BxPC3 was in second and third place, respectively.